Predictive Science, Inc.

STATUS OF CORHEL AND SUPPORTING RESEARCH FOR CORONAL AND HELIOSPHERIC MODELING

Zoran Mikić
Pete Riley
Jon A. Linker
Roberto Lionello
Viacheslav Titov

Predictive Science, Inc., San Diego, CA, USA

Dusan Odstrcil

NASA GSFC, Greenbelt, MD, USA

Presented at the 5th CCMC Workshop, Key Largo, FL, January 25–29, 2010

Supported by NASA's Heliophysics Theory & LWS Programs, and NSF/CISM

WHAT IS CORHEL?

- CORHEL is a suite of models to study coronal and heliospheric solar wind structure
- Contains three coronal models (WSA, MAS polytropic, MAS thermodynamic)
- Contains two heliospheric models (Enlil and MAS)
- It been used by CISM to study the accuracy of solar wind estimates (Owens *et al*. 2008)
- Version 4.2 has been implemented at CCMC
- CCMC has tailored the implementation to suit their system
- Version 4.3 is currently under development
- CORHEL is a research model
- Used at CCMC, CISM, and AFRL
- It can be useful in developing space weather prediction models
- It might eventually mature into an operational tool

FEATURES OF CORHEL

- Driven by photospheric magnetograms (6 observatories)
- Intended to be user friendly
- Also runs in command-line mode (for expert users)
- Includes post-processing and visualization tools (Visual & SolarView)
- Includes a web-based interactive magnetogram processor
  - interactive display of the raw magnetogram
  - interactive control of pole fitting and smoothing
  - interactive display of the processed magnetogram
- Can run cone model CMEs
- It has our implementation of the WSA model
  - consistent processing between WSA and MAS inputs
  - allows for meaningful comparisons between WSA and MHD models, and comparison of different magnetograms

CORHEL Suite for Coronal and Heliospheric Modeling

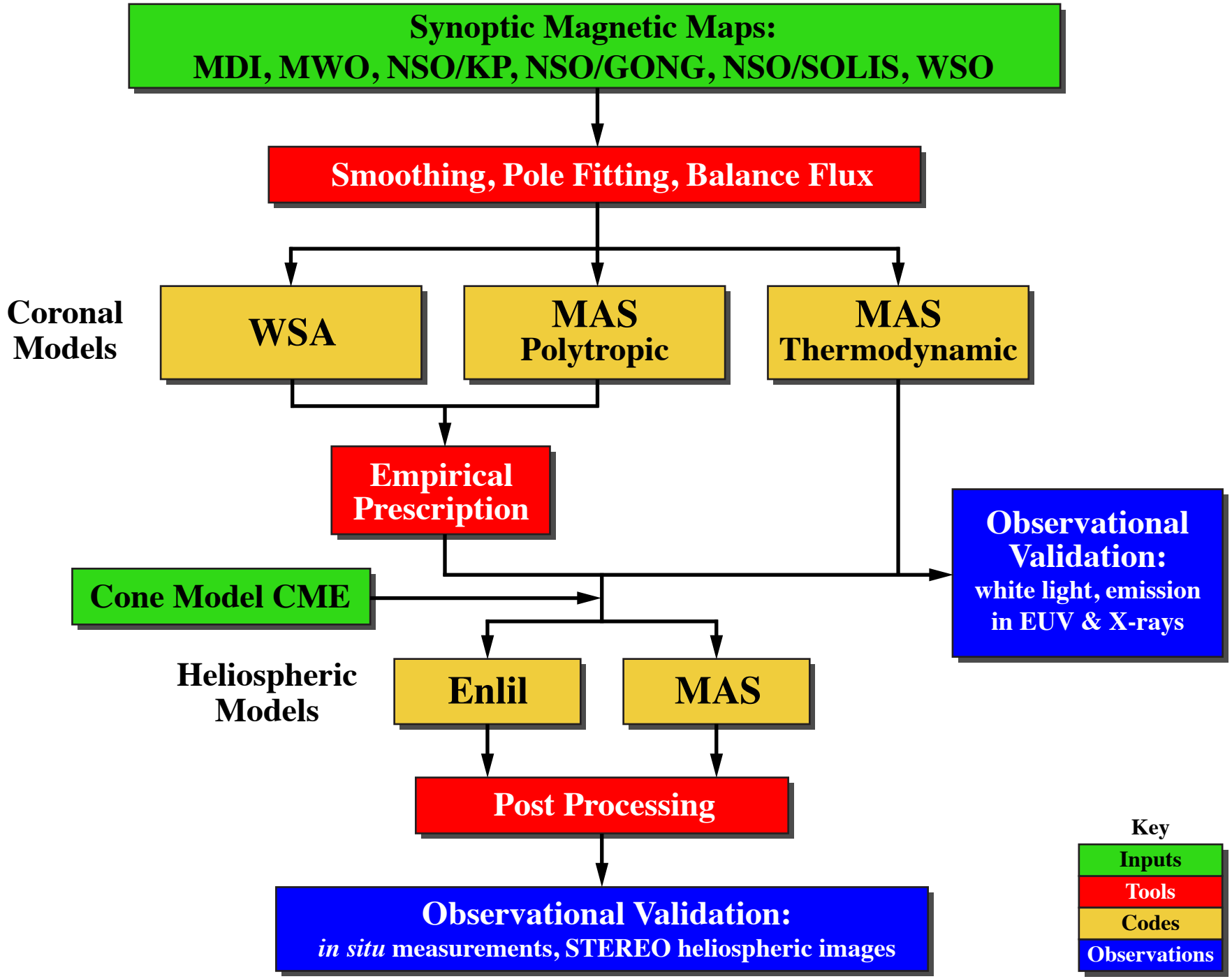

RESISTIVE MHD EQUATIONS
(POLYTROPIC MODEL)

$$\nabla \times \mathbf{B} = \frac{4\pi}{c}\mathbf{J}$$

$$\nabla \times \mathbf{E} = -\frac{1}{c}\frac{\partial \mathbf{B}}{\partial t}$$

$$\mathbf{E} + \frac{1}{c}\mathbf{v} \times \mathbf{B} = \eta \mathbf{J}$$

$$\frac{\partial \rho}{\partial t} + \nabla \cdot (\rho \mathbf{v}) = 0$$

$$\rho\left(\frac{\partial \mathbf{v}}{\partial t} + \mathbf{v} \cdot \nabla \mathbf{v}\right) = \frac{1}{c}\mathbf{J} \times \mathbf{B} - \nabla p - \nabla p_w + \rho \mathbf{g} + \nabla \cdot (\nu \rho \nabla \mathbf{v})$$

$$\frac{\partial p}{\partial t} + \nabla \cdot (p\mathbf{v}) = -(\gamma - 1) p \nabla \cdot \mathbf{v}$$

with $\gamma = 1.05$, and WKB Alfvén wave pressure p_w evolution

RESISTIVE MHD EQUATIONS
(IMPROVED ENERGY TRANSPORT)

$$\nabla \times \mathbf{B} = \frac{4\pi}{c}\mathbf{J}$$

$$\nabla \times \mathbf{E} = -\frac{1}{c}\frac{\partial \mathbf{B}}{\partial t}$$

$$\mathbf{E} + \frac{1}{c}\mathbf{v} \times \mathbf{B} = \eta \mathbf{J}$$

$$\frac{\partial \rho}{\partial t} + \nabla \cdot (\rho \mathbf{v}) = 0$$

$$\rho\left(\frac{\partial \mathbf{v}}{\partial t} + \mathbf{v} \cdot \nabla \mathbf{v}\right) = \frac{1}{c}\mathbf{J} \times \mathbf{B} - \nabla p - \nabla p_w + \rho \mathbf{g} + \nabla \cdot (\nu \rho \nabla \mathbf{v})$$

$$\frac{\partial p}{\partial t} + \nabla \cdot (p\mathbf{v}) = (\gamma - 1)(-p\nabla \cdot \mathbf{v} - \nabla \cdot \mathbf{q} - n_e n_p Q(T) + H)$$

$$\mathbf{q} = -\kappa_{\parallel} \hat{\mathbf{b}}\hat{\mathbf{b}} \cdot \nabla T \qquad \text{(Close to the Sun, } r \lesssim 10R_S\text{)}$$

$$\mathbf{q} = 2\alpha n_e T\, \hat{\mathbf{b}}\hat{\mathbf{b}} \cdot \mathbf{v}/(\gamma - 1) \qquad \text{(Far from the Sun, } r \gtrsim 10R_S\text{)}$$

with $\gamma = 5/3$, and WKB Alfvén wave pressure p_w evolution

Various Applications

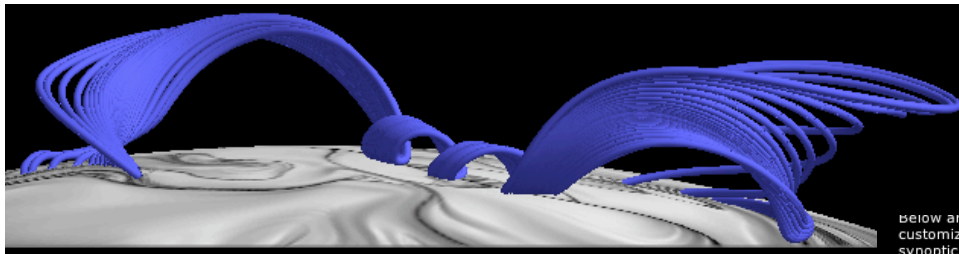

This web application helps users process synoptic maps and generate the input file for running so
software package.

Enter a Carrington rotation or a date of interest and click on the Next button to obtain and proces
observatories.

Carrington rotation: 2084

Date: 05 / 30 / 2009

Observatories:
- GONG
- Kitt Peak
- MDI
- Mount Wilson
- SOLIS
- Wilcox

Next

Below are the raw and the filtered synoptic maps from **Carrington rotation 2084**. Enter different values for each parameter to customize the filtered synoptic map. Once you get the desired synoptic map, click on the Download button to download the filtered synoptic map, which can be used as an input to run solar corona model using CORHEL software package.

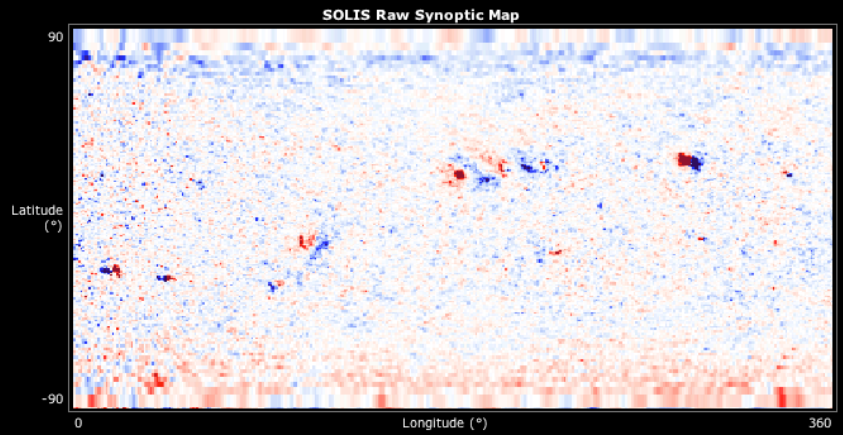

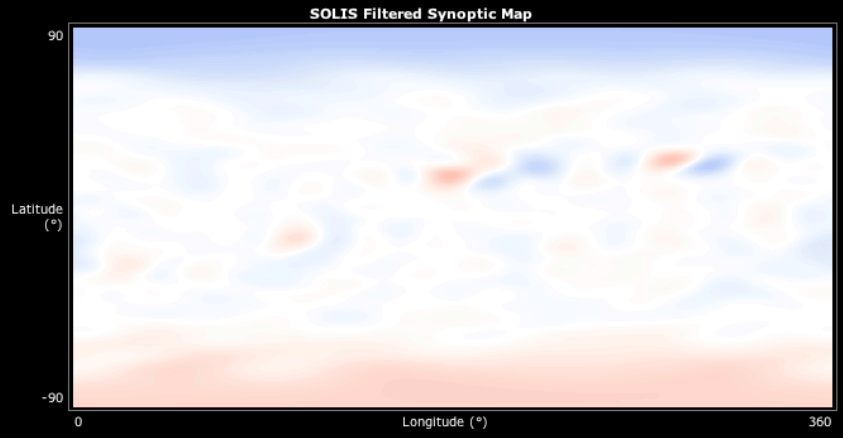

Polefitting - TH0: 0.25 radians

Polefitting - TH1: 0.45 radians

Polefitting - THR: 0.35 radians

Minimum scale value: -50 Gauss

Maximum scale value: 50 Gauss

Palette: Blue Red

Raw Synoptic Map: CR1913

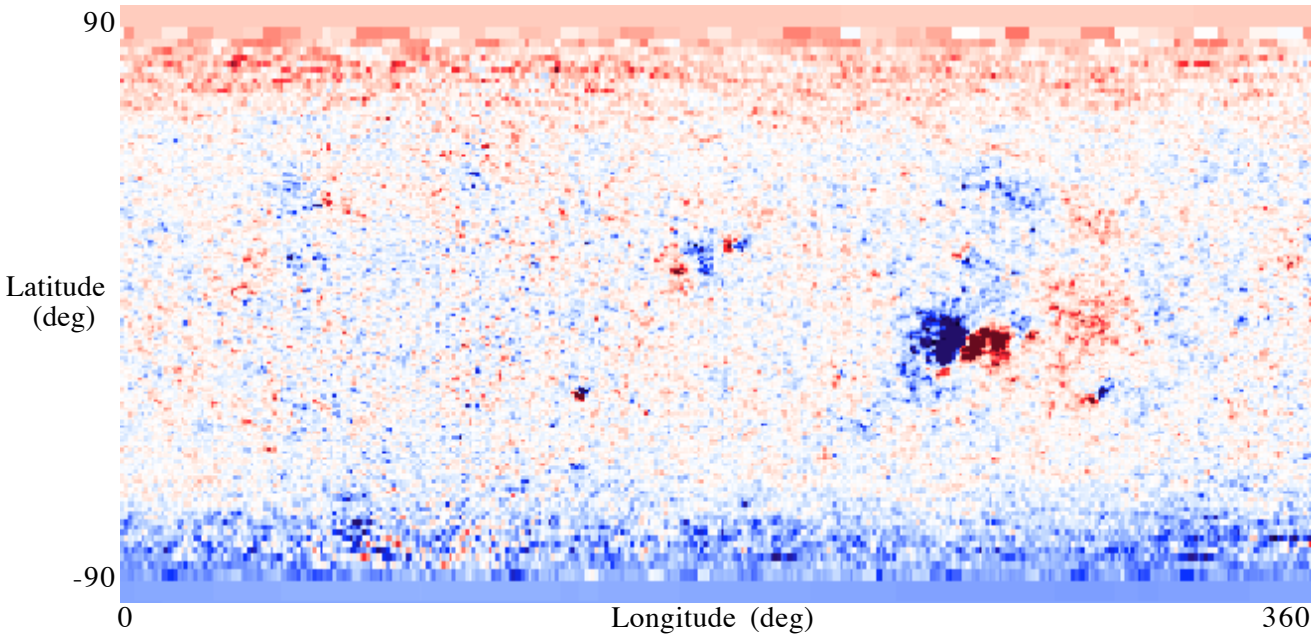

Filtered Synoptic Map: CR1913

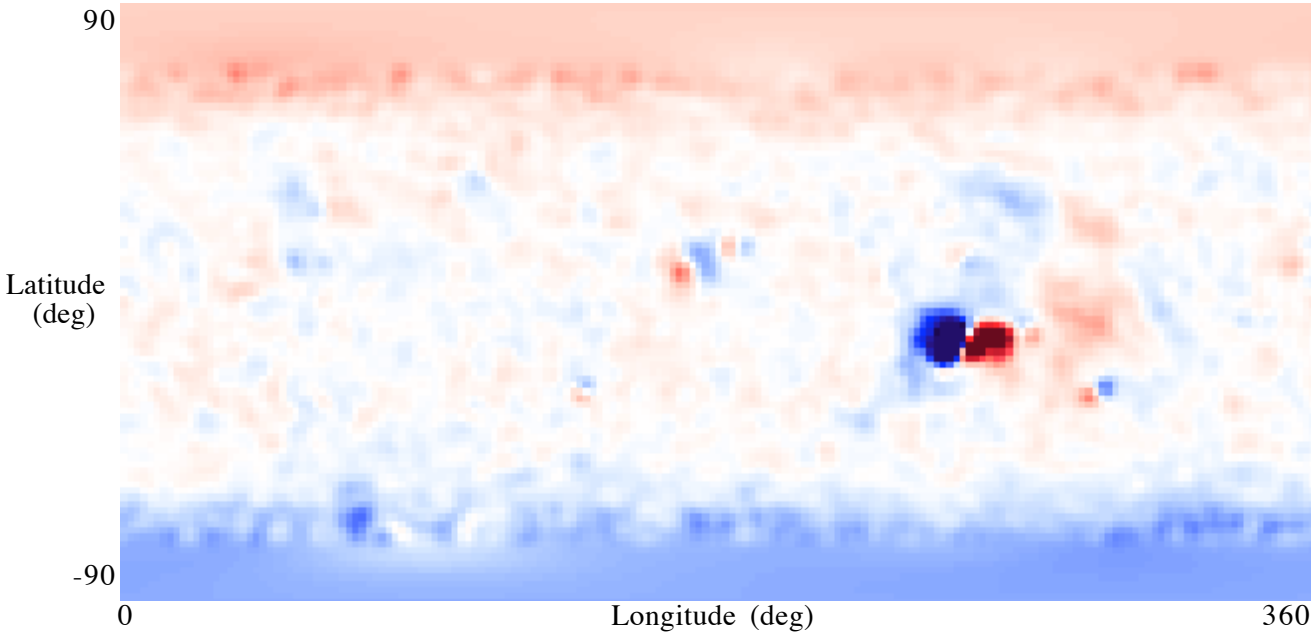

Radial Magnetic Field Magnitude [Gauss]

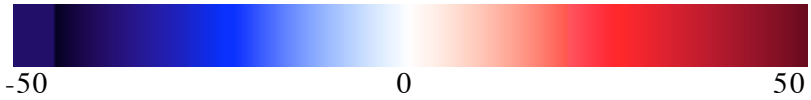

WSA Solar Wind Speed: CR1913

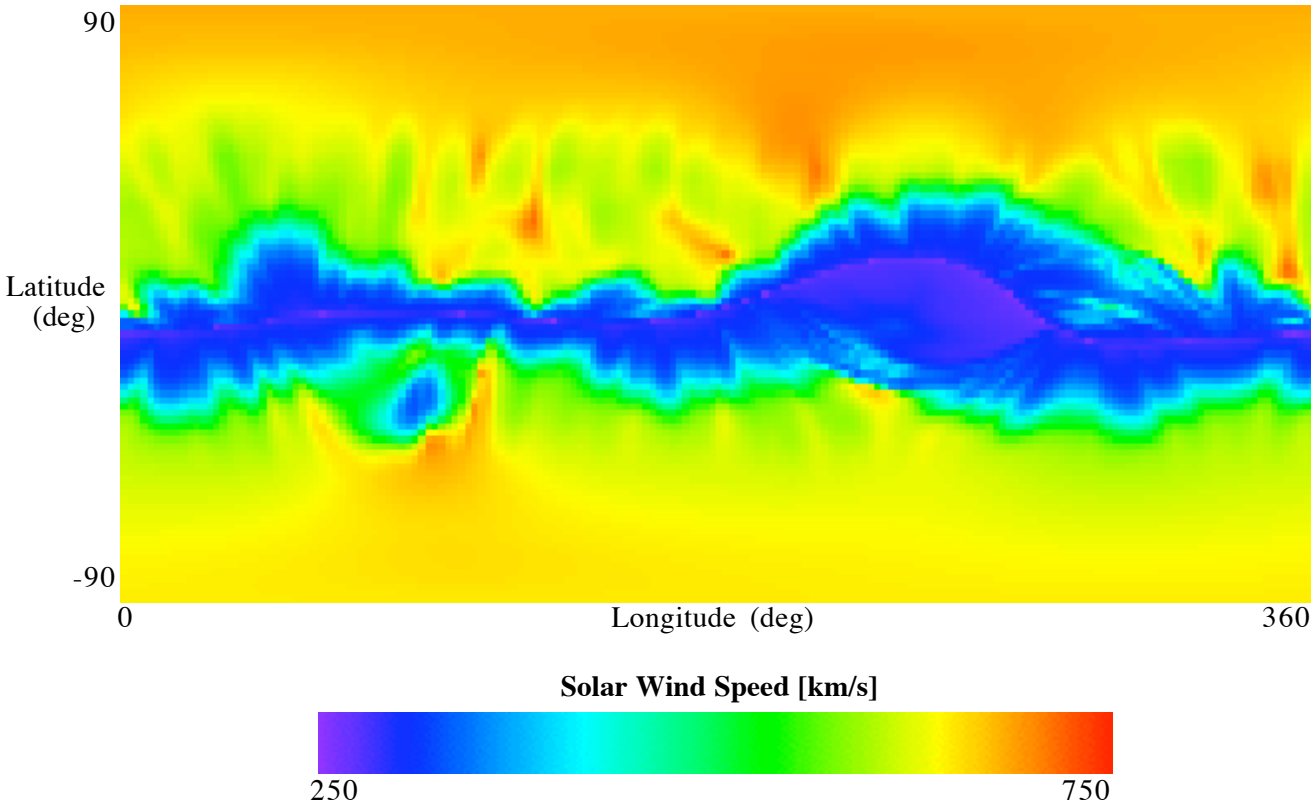

Coronal Hole Map: CR1913

Carrington Rotation 2068 (April 16 – May 13, 2008)
SOLIS LOS Magnetogram

Coronal Model: **WSA**
Heliospheric Model: **MAS**

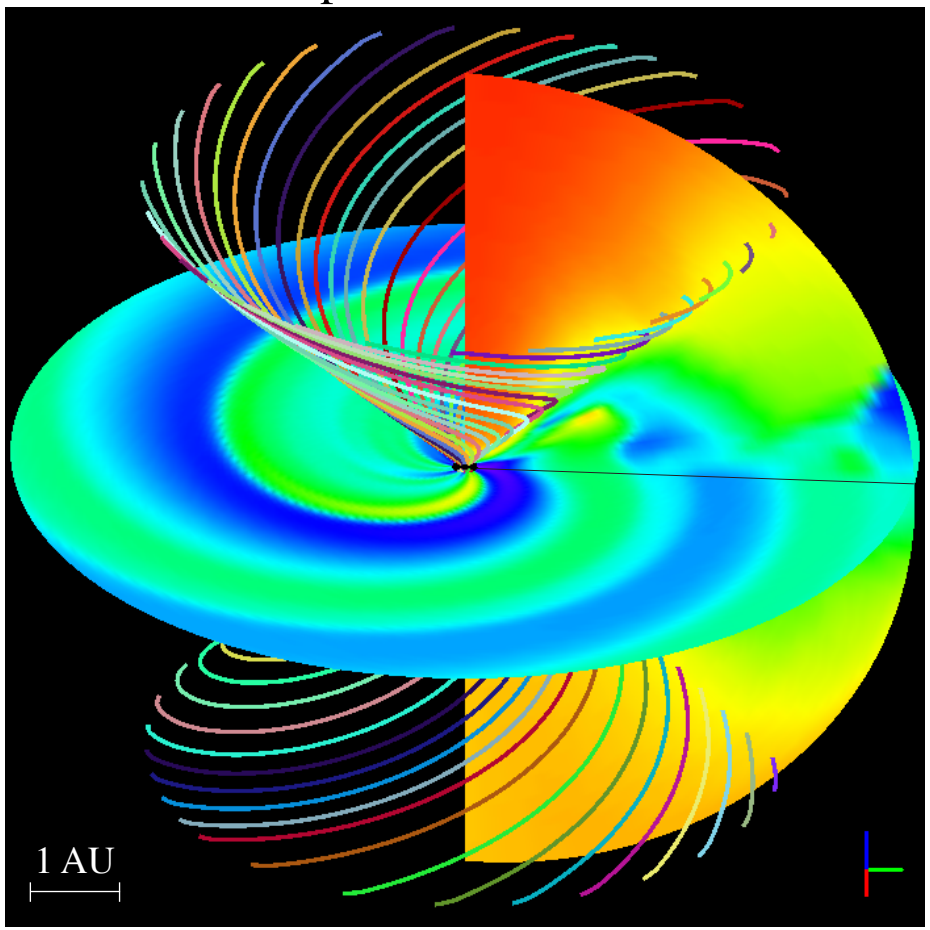

Coronal Model: **MAS**
Heliospheric Model: **MAS**

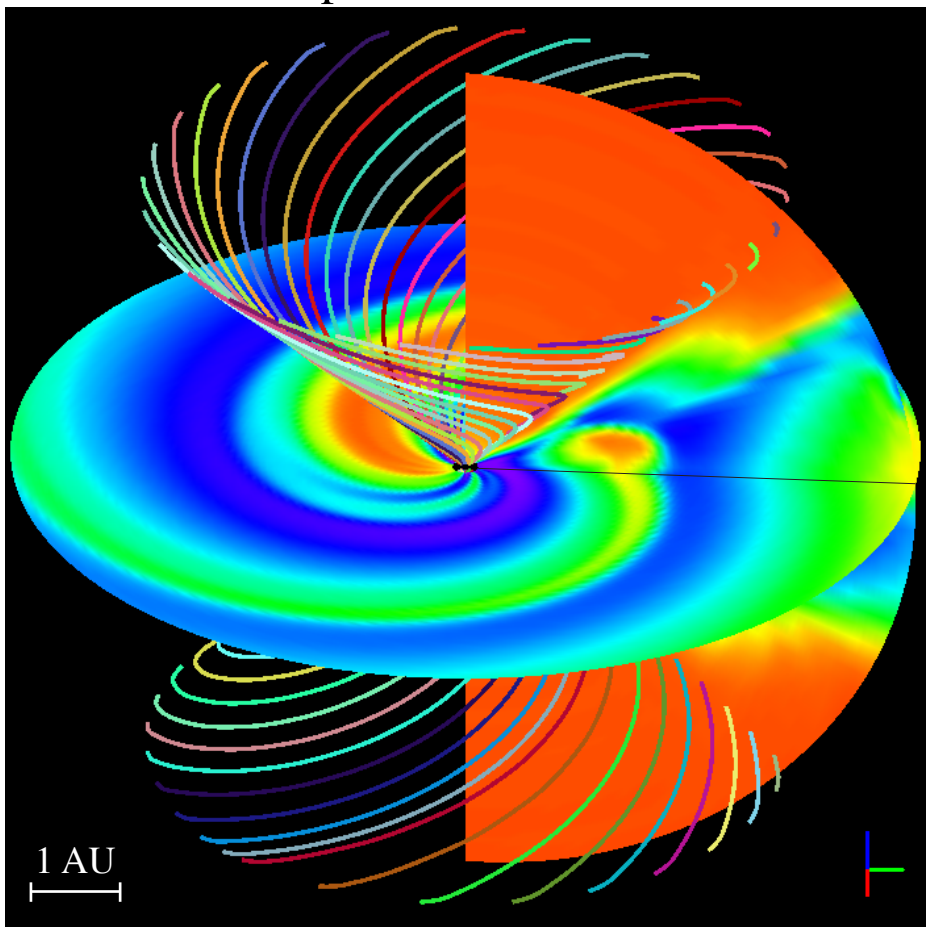

Radial Velocity [km/s]

300 400 500 600 700 800

Cone Model CME Simulations

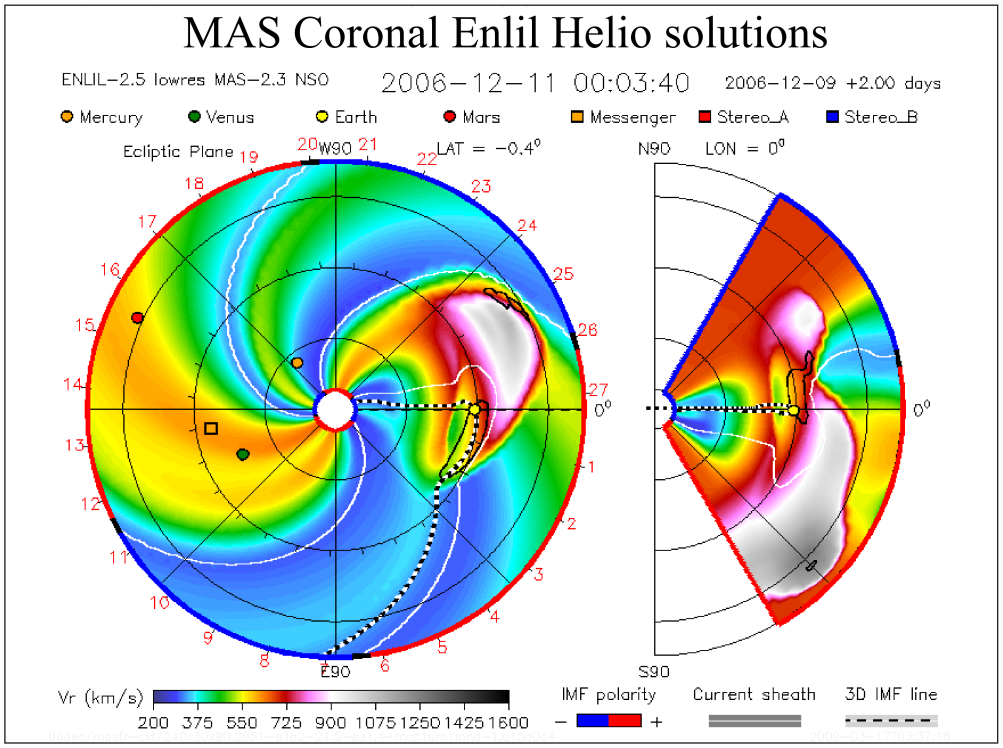

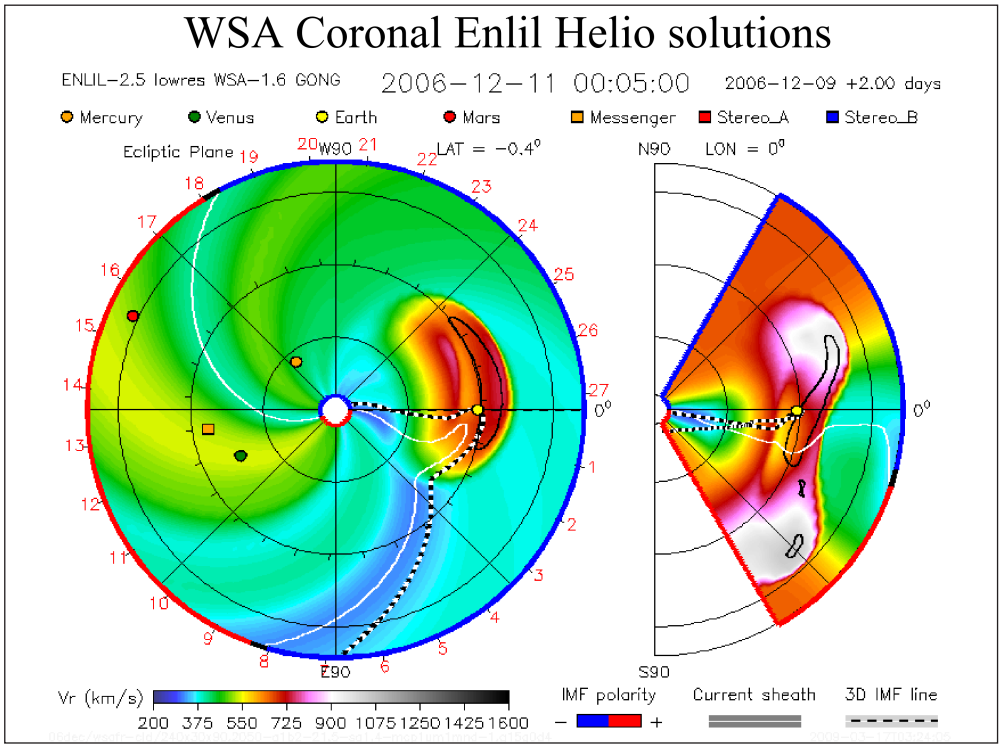

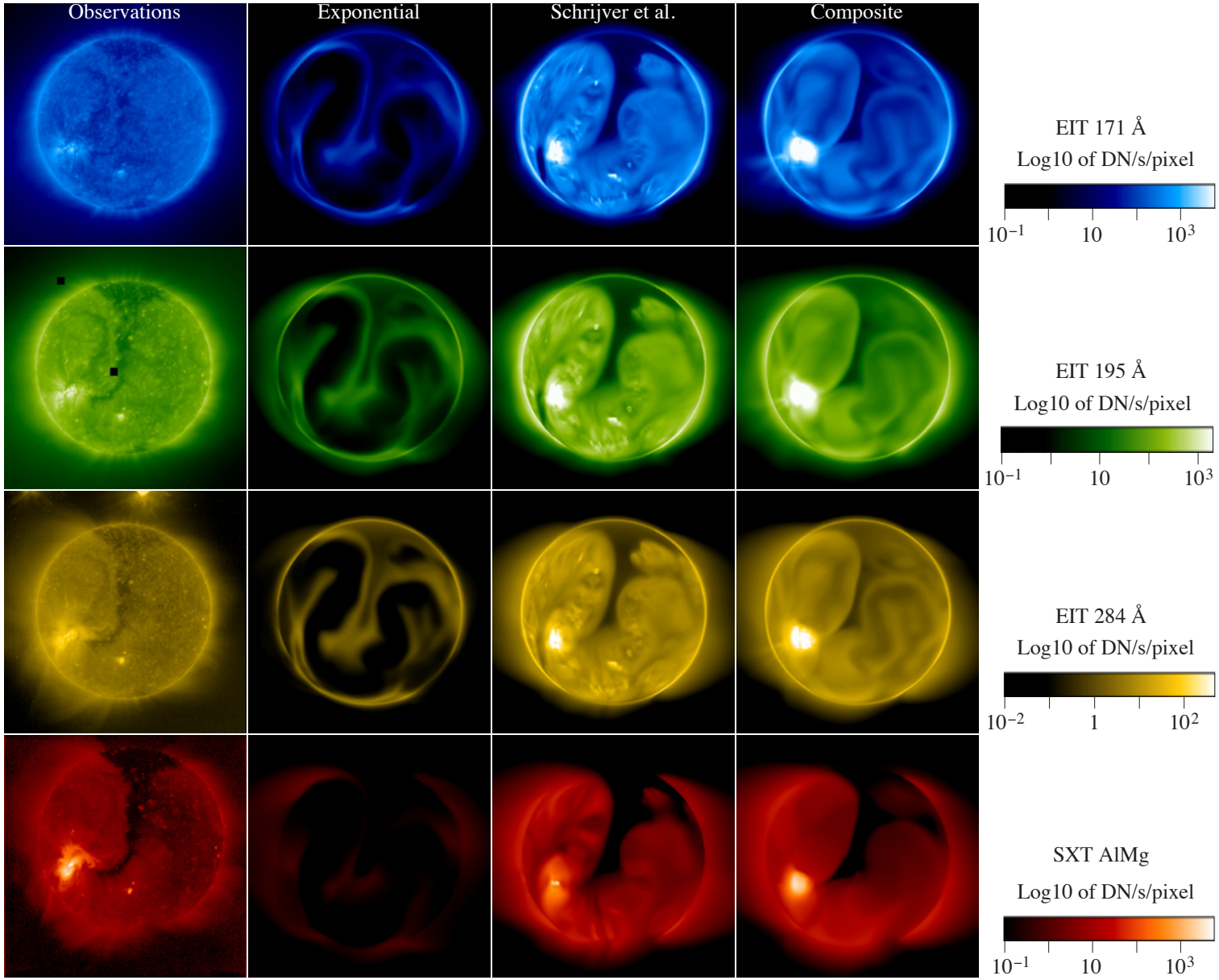

Figure 8. Comparison of observed and synthetic emission images. The first column shows the observed emission, each remaining column shows the computed emission for models 1, 2, and 3 (see Section 2.2). Rows show emission in the EIT 171, 195, and 284 Å band and in the SXT AlMg configuration. The observations were taken on 1996 August 27 at 00:00:13, 00:24:05, 01:05:19, and 02:11:33 UT, respectively. The resolution is 1024^2 pixels for the EIT images and 512^2 pixels for the SXT. The computed emission images were calculated for 00:30:00 UT, corresponding to a central meridian Carrington longitude of 296°.

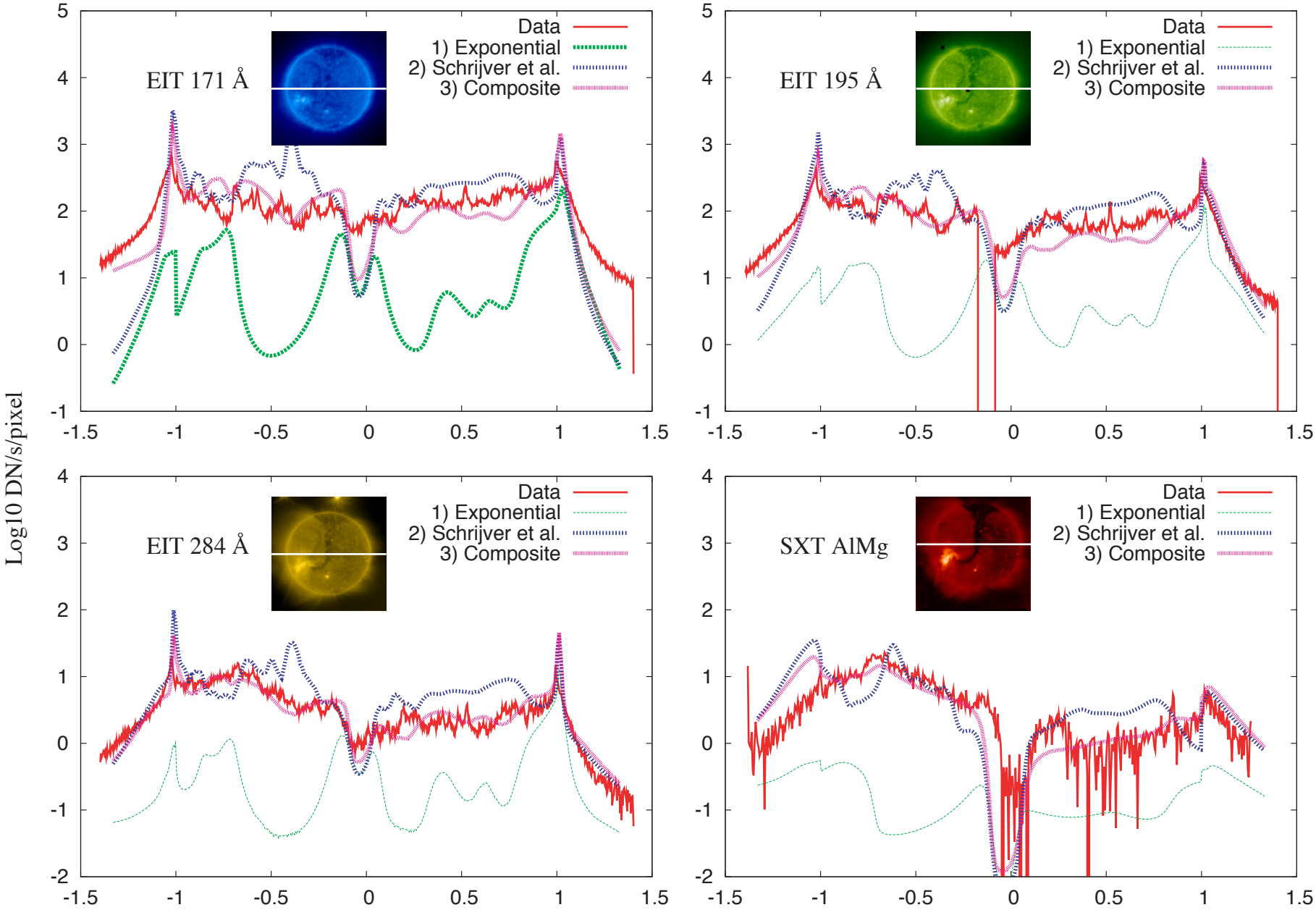

Figure 9. Comparison of observed and synthetic emission along an equatorial cut. The synthetic emission was obtained using models 1, 2, and 3 of Section 2.2.

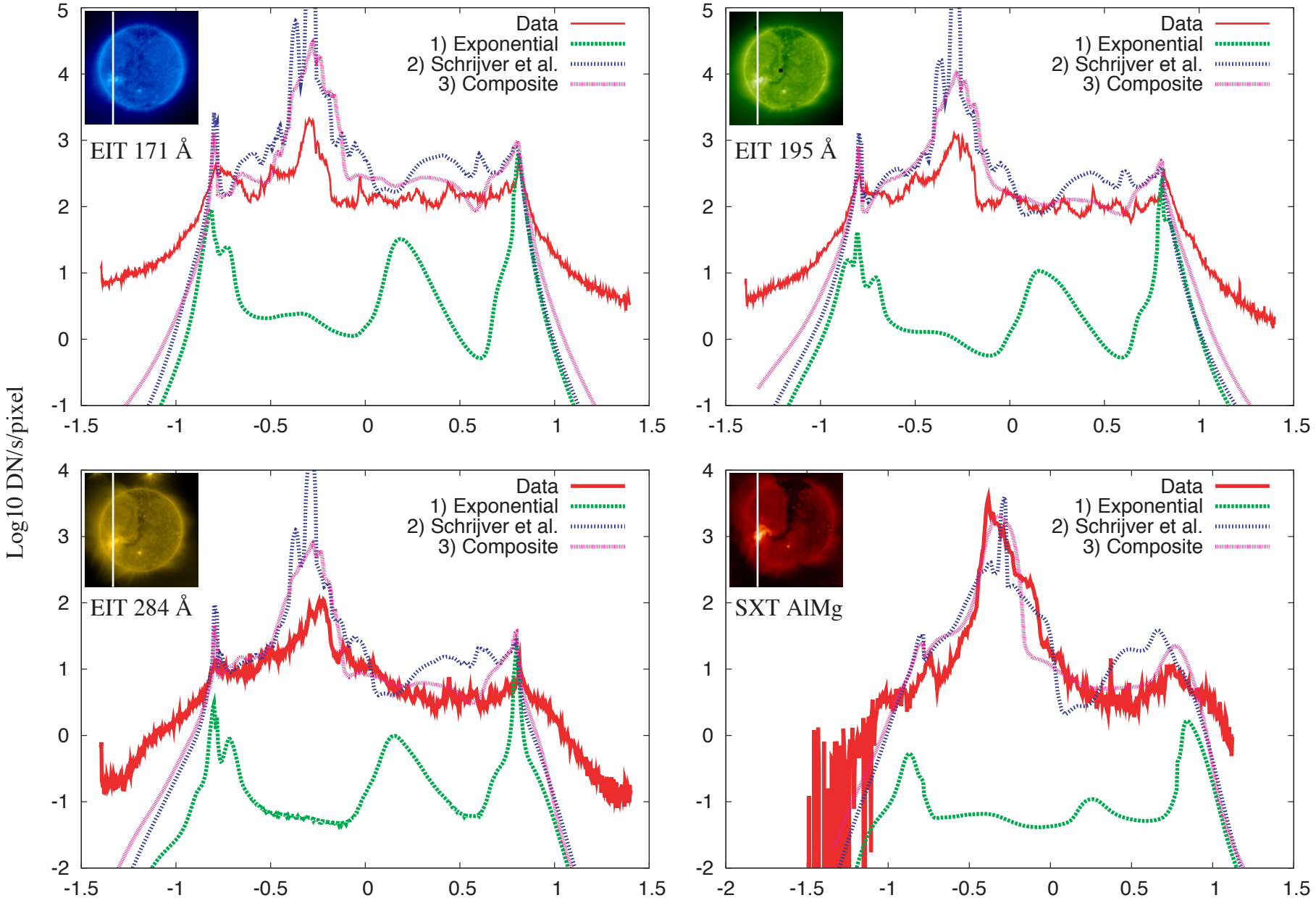

Figure 10. Comparison of observed and synthetic emission along a cut intersecting the active region. The synthetic emission was obtained using models 1, 2, and 3 of Section 2.2.

Comparison of Simulated and Observed Emission for Four Different Time Periods

Observed Emission on May 11, 1997 near 01:00UT [Log_{10}DN/s]

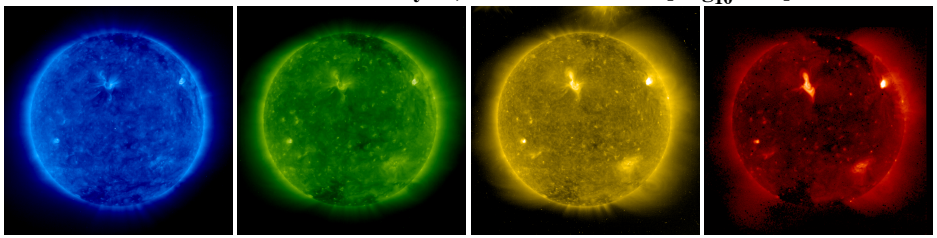

Simulated SOHO EIT and Yohkoh SXT Emission [Log_{10}DN/s]

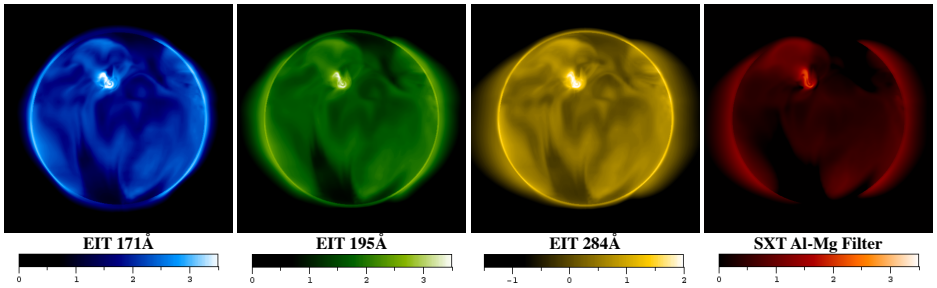

Observed Emission on May 13, 2005 near 11:36UT [Log_{10}DN/s]

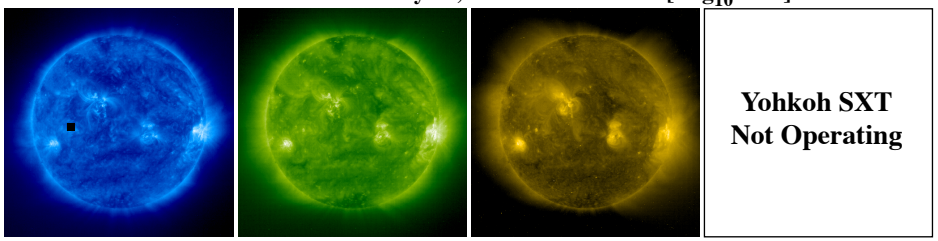

Simulated SOHO EIT and Yohkon SXT Emission [Log_{10}DN/s]

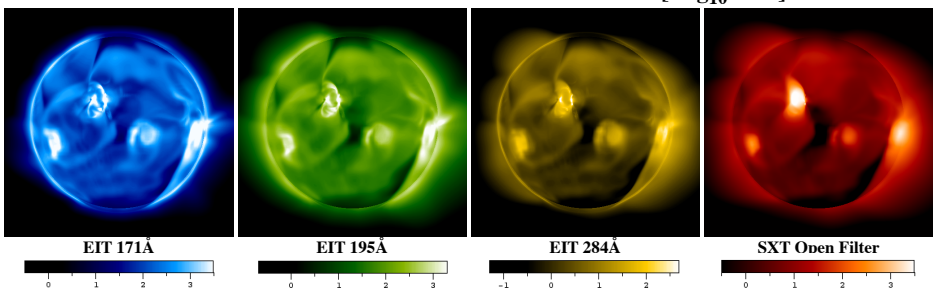

Observed Emission on September 20, 2007 near 13:00UT [Log_{10}DN/s]

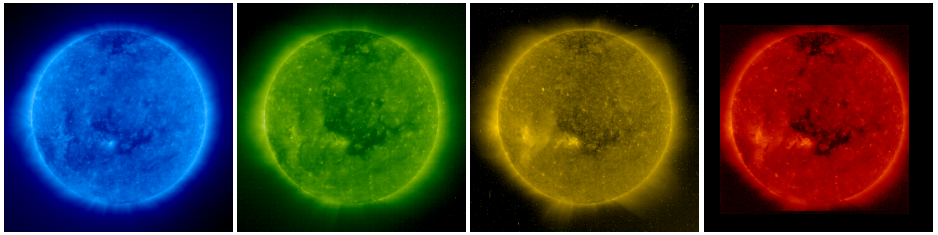

Simulated SOHO EIT and Yohkon SXT Emission [Log_{10}DN/s]

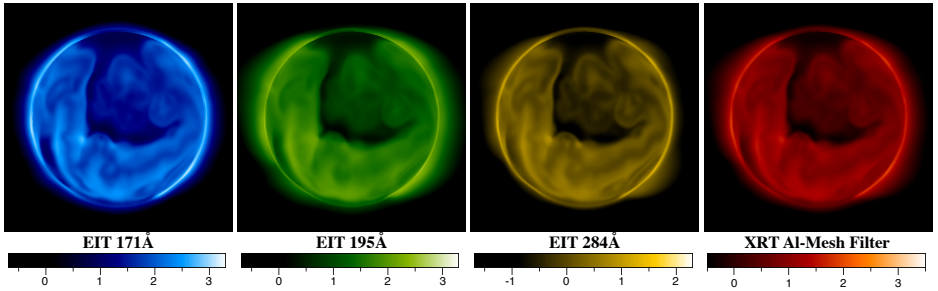

Observed Emission on July 19, 2008 near 15:00UT [Log_{10}DN/s]

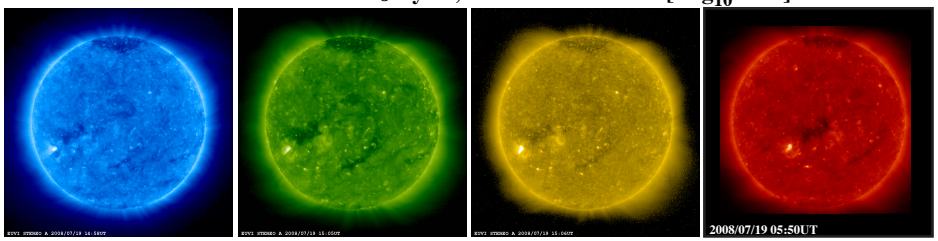

Simulated STEREO A EUVI and Hinode XRT Emission [Log_{10}DN/s]

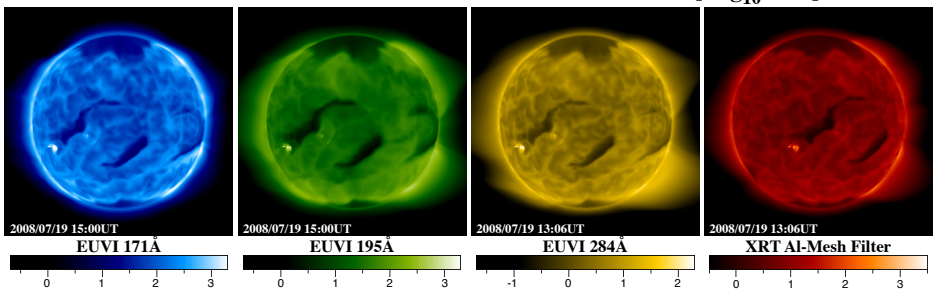

August 1, 2008 Total Solar Eclipse

Predicted Magnetic Field Lines

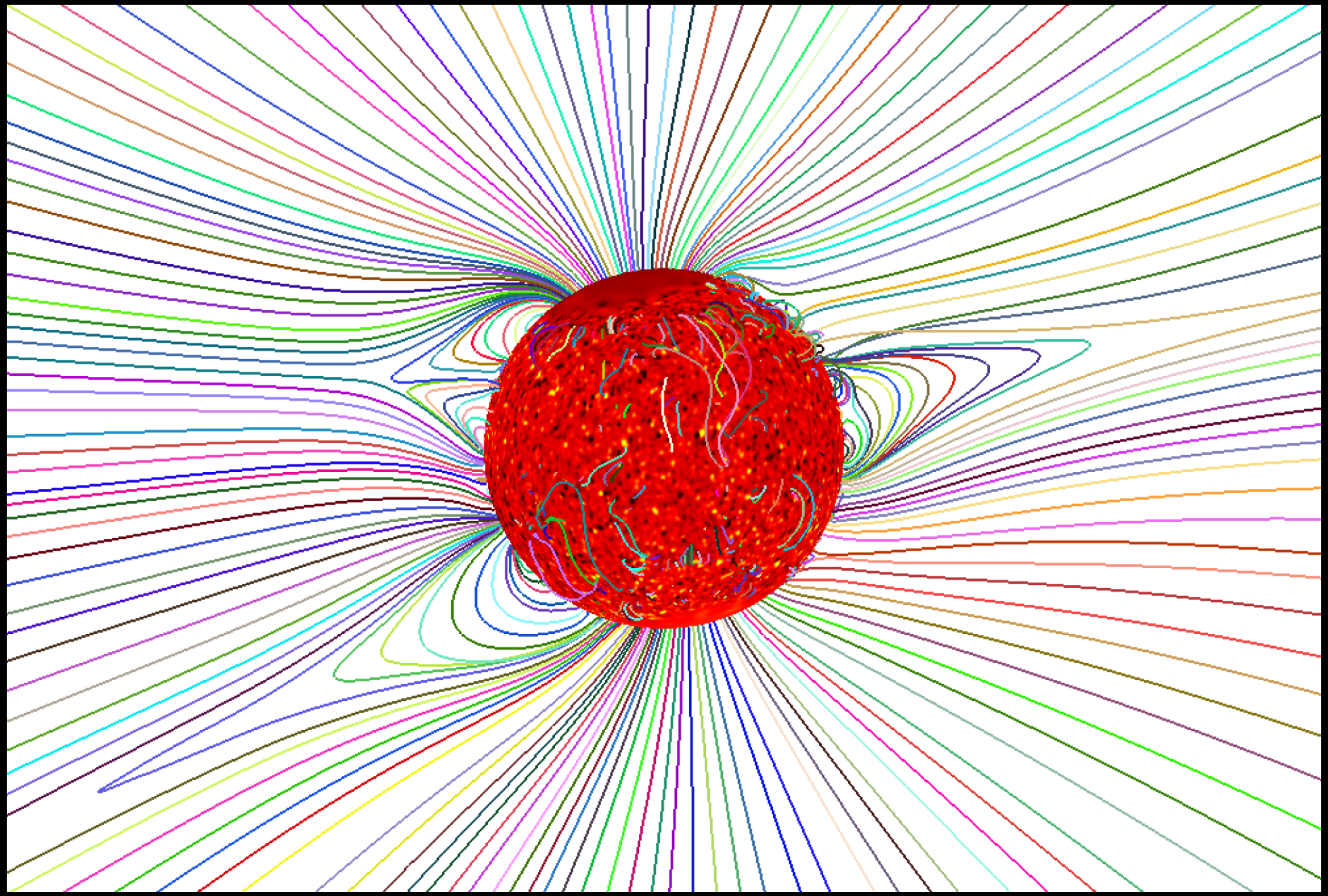

August 1, 2008 Total Solar Eclipse

Predicted Polarization Brightness

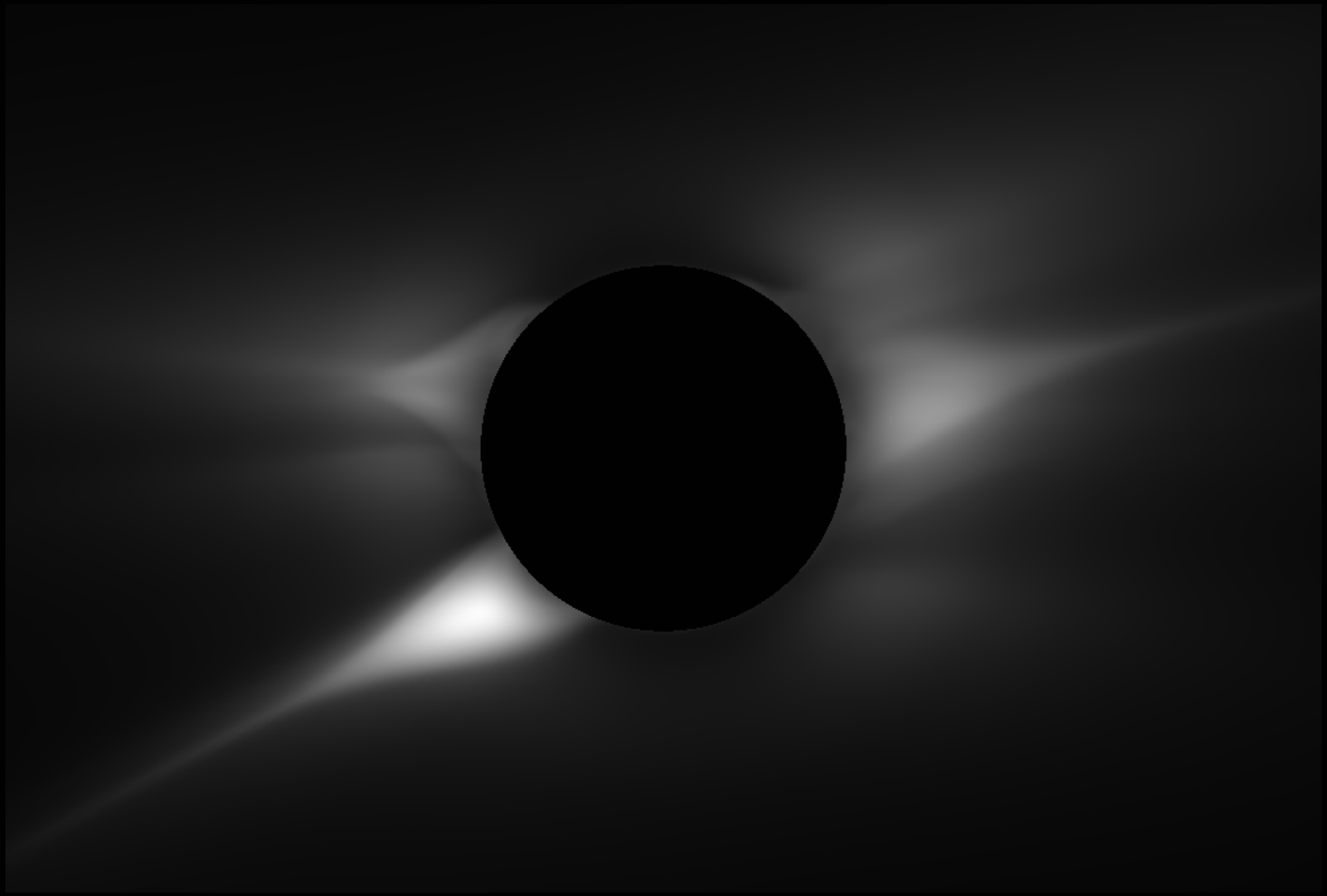

August 1, 2008 Total Solar Eclipse

Image from Mongolia (Druckmüller, Aniol, & Rušin)

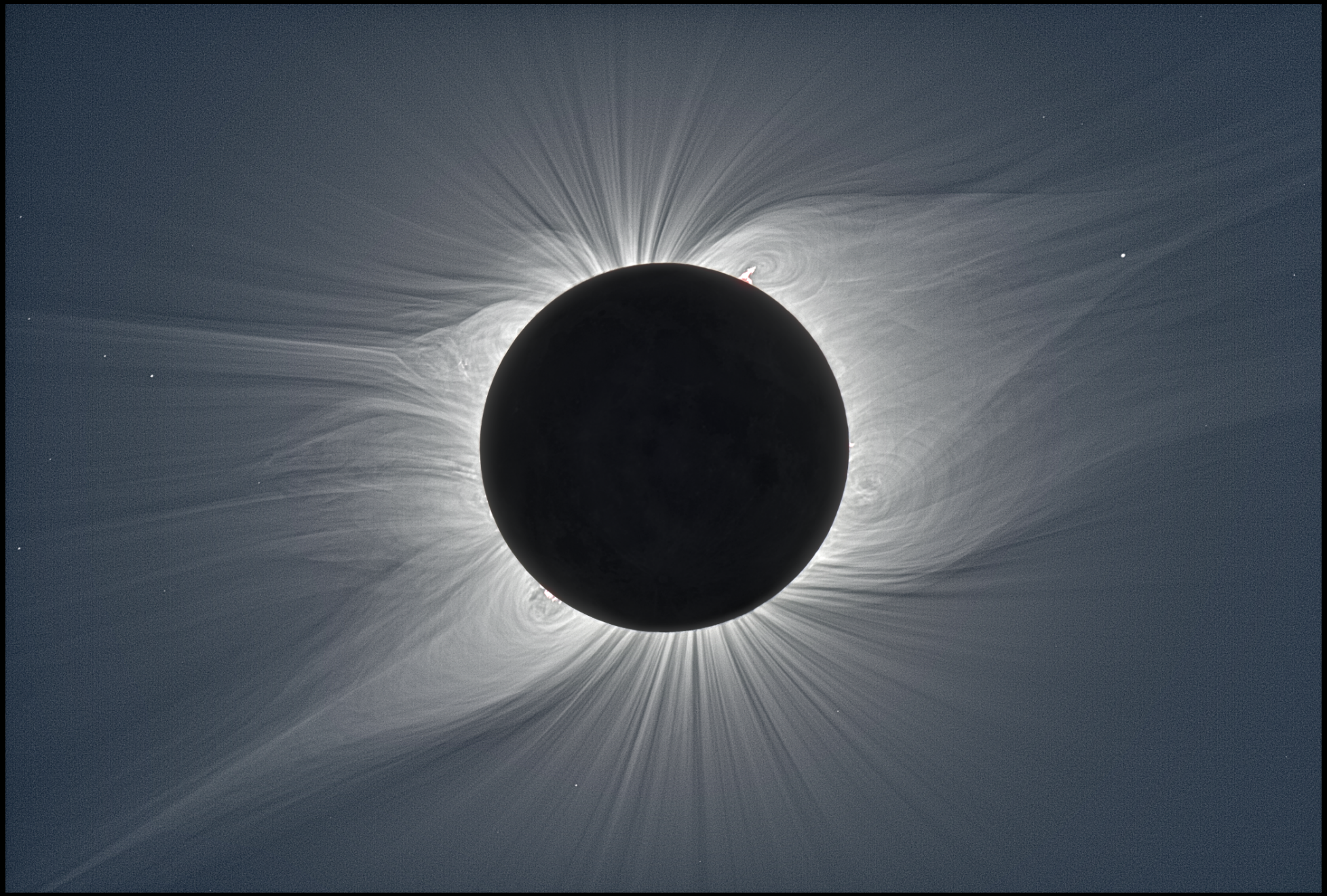

August 1, 2008 Total Solar Eclipse

Image from Mongolia ⟷ Simulated pB

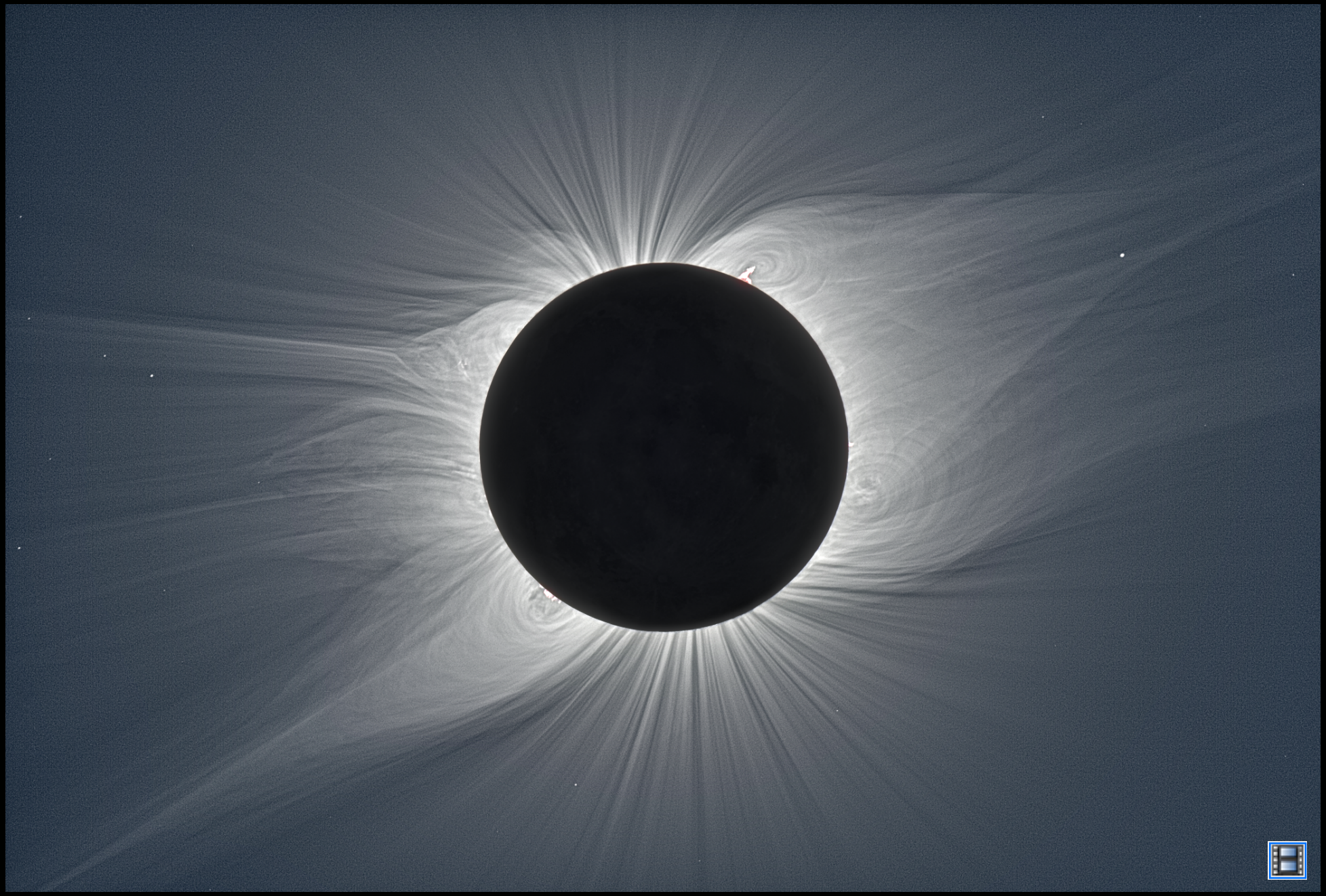

August 1, 2008 Total Solar Eclipse

Image from Mongolia ⟷ Field Lines

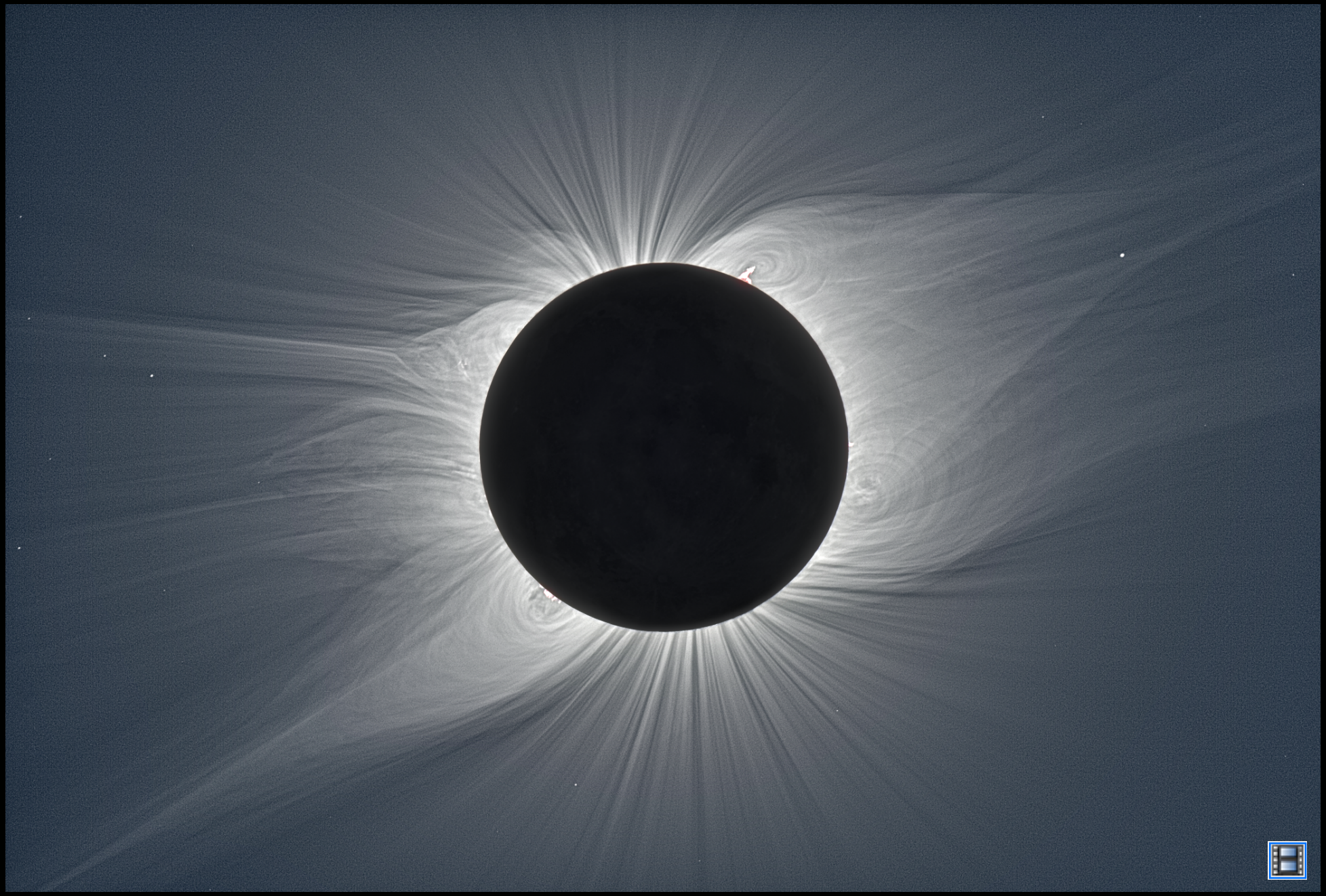

Observed vs. Simulated STEREO EUVI A & B 195Å Emission

June 25 – July 22, 2008

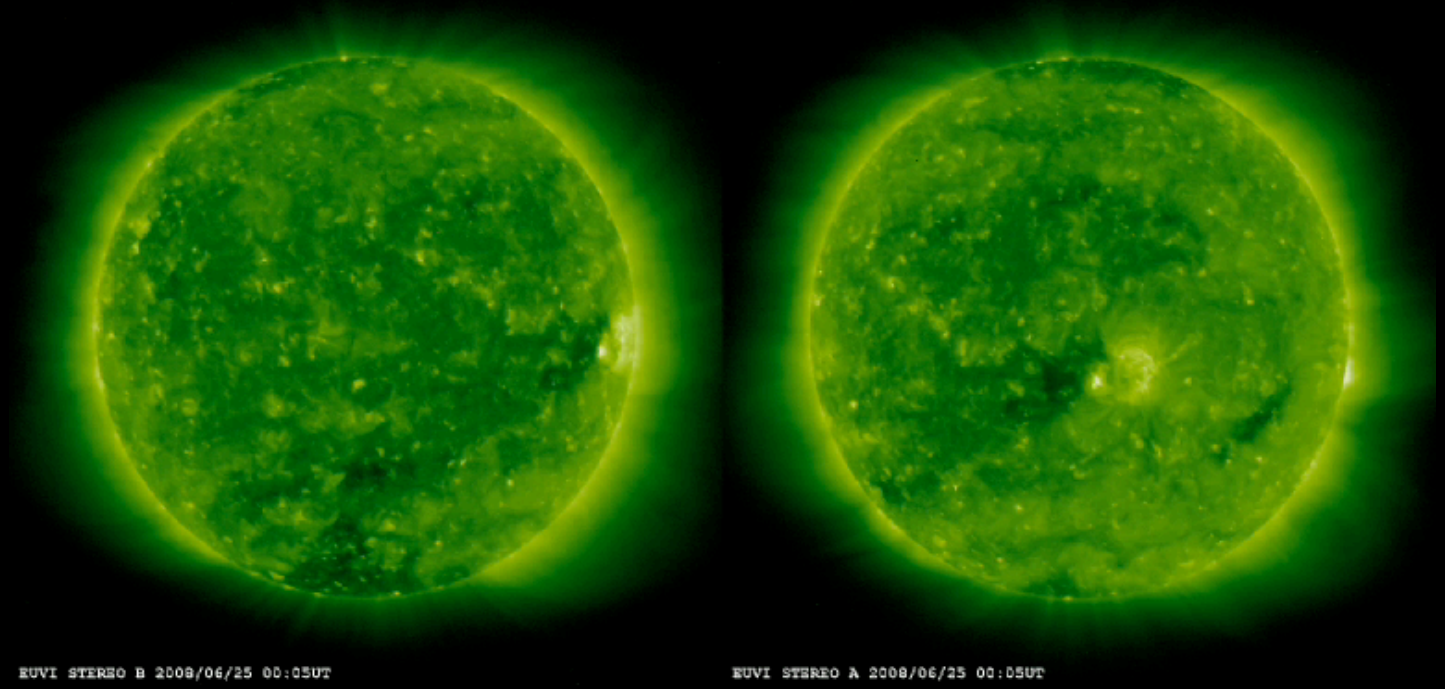

12 May 1997 CME Eruption

20 minutes after eruption **38 minutes after eruption** **62 minutes after eruption**

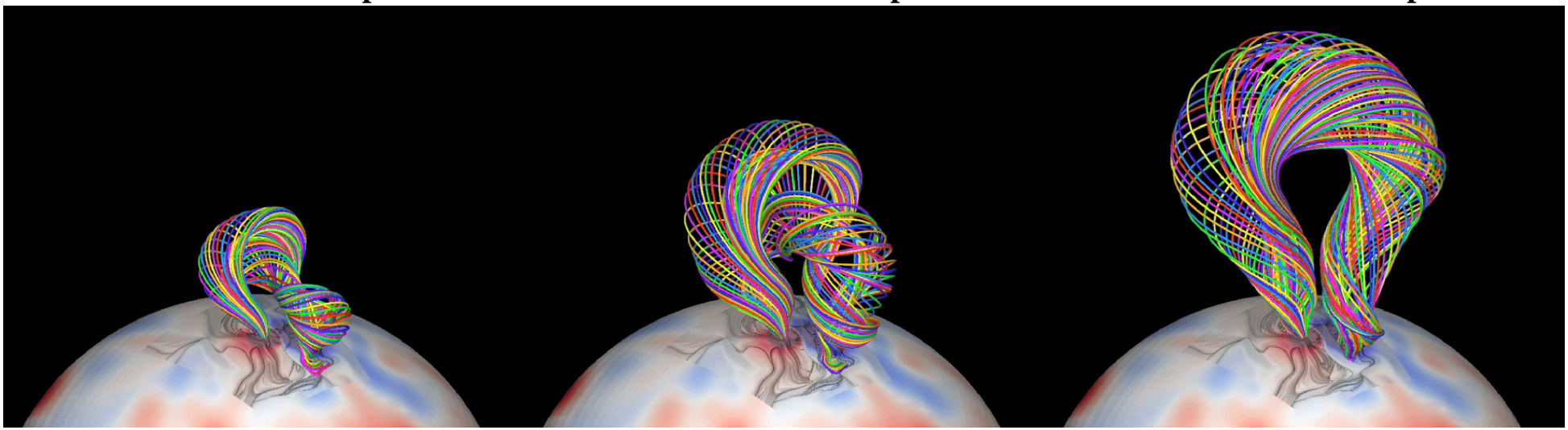

May 12, 1997 CME Event: Prominence Formation

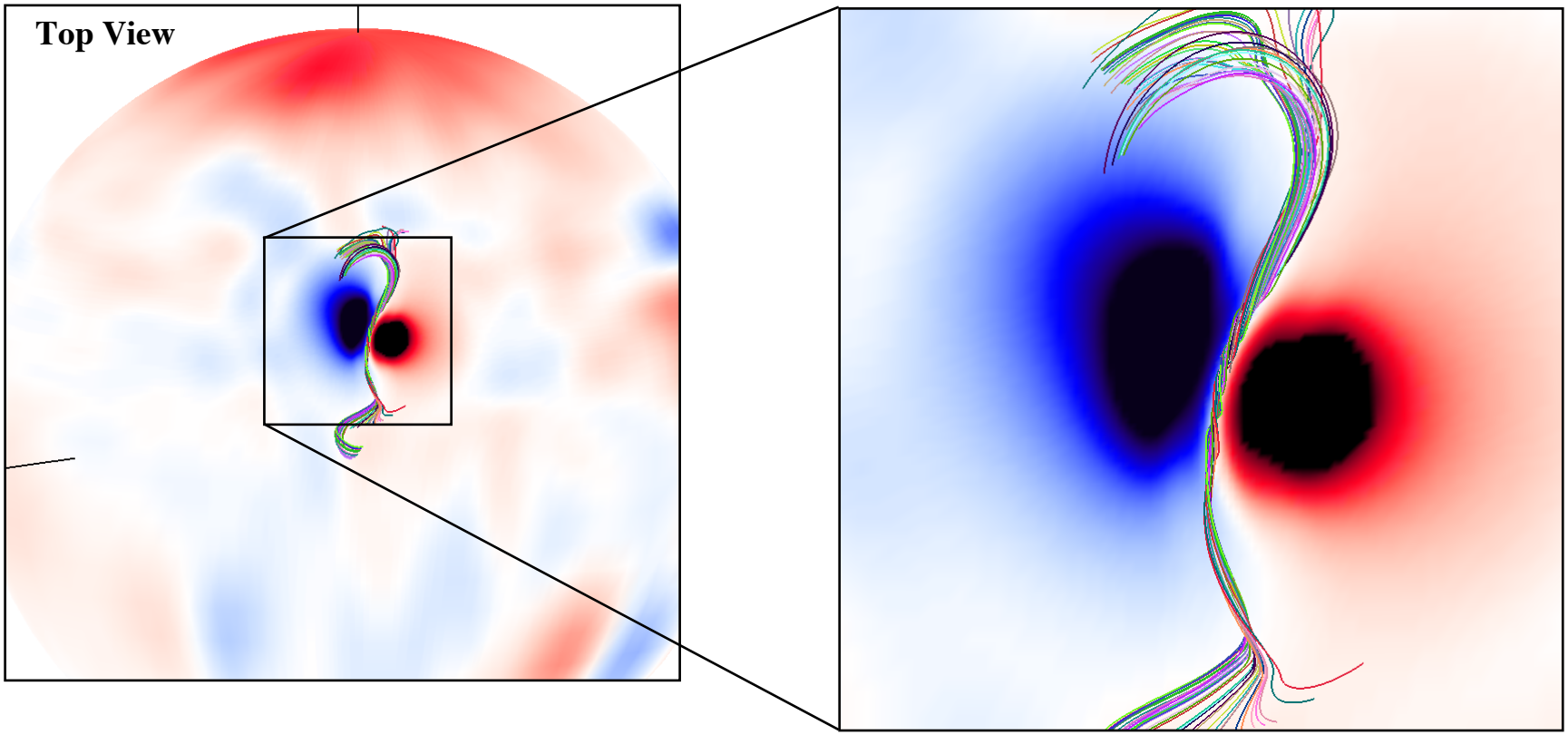

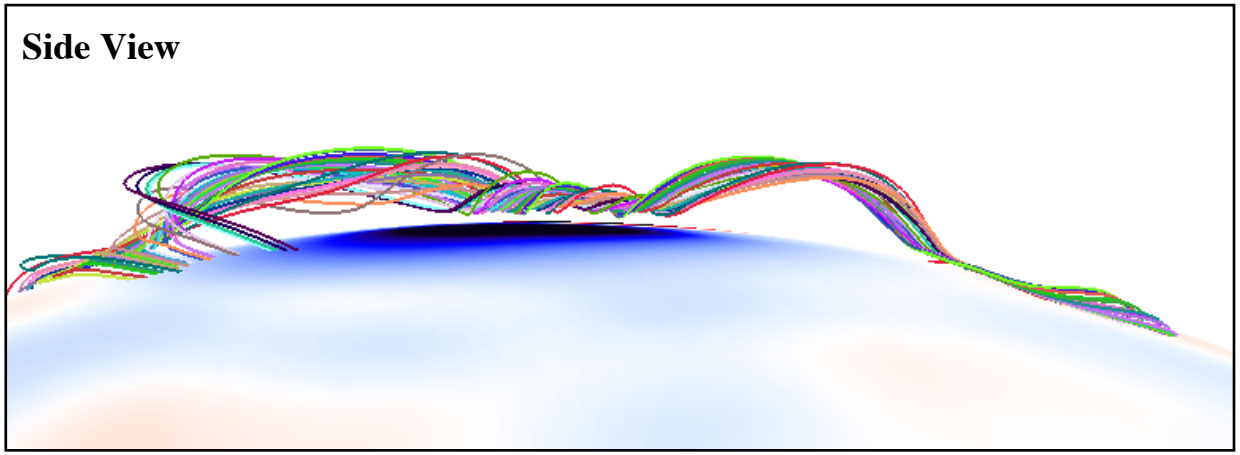

ar88dephi05

Formation and Eruption of a Prominence by Flux Cancellation

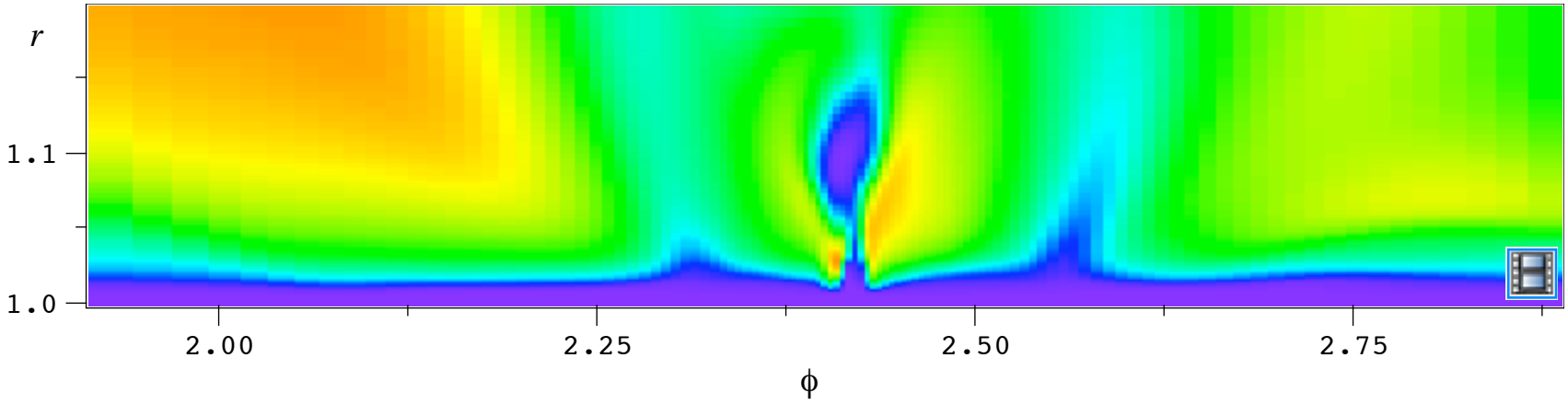

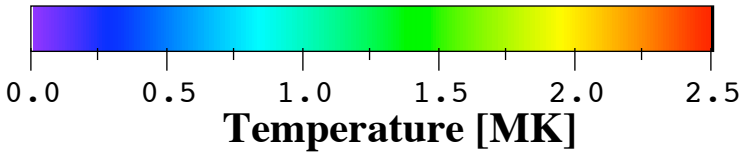

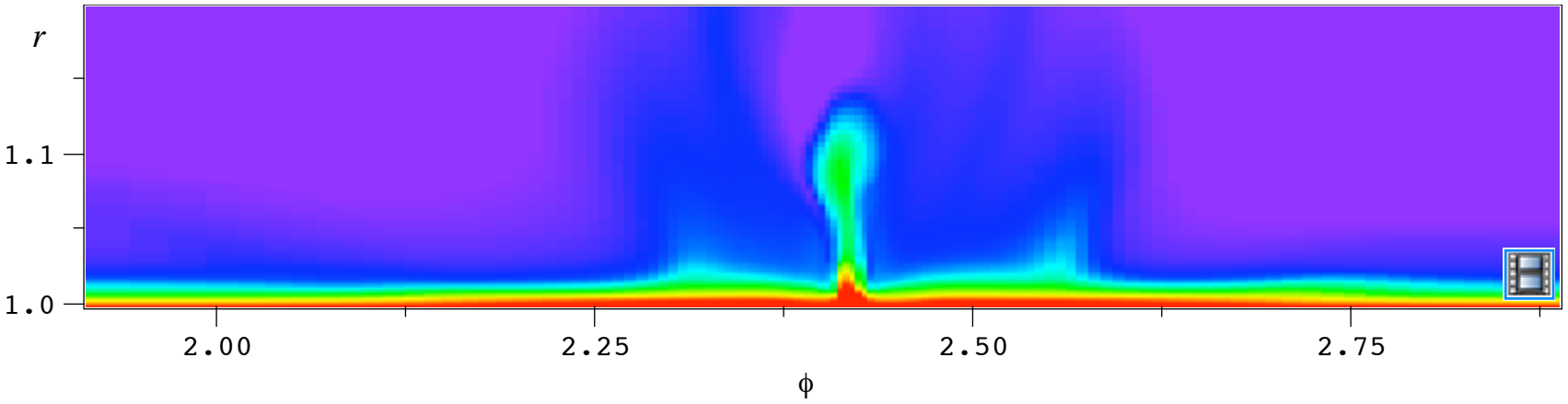

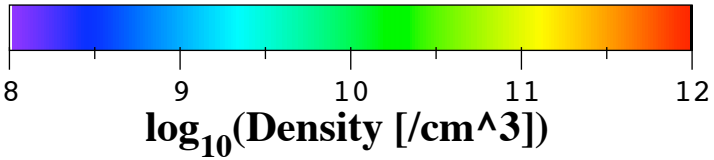

ar88dephi05+06

Magnetic Field Lines

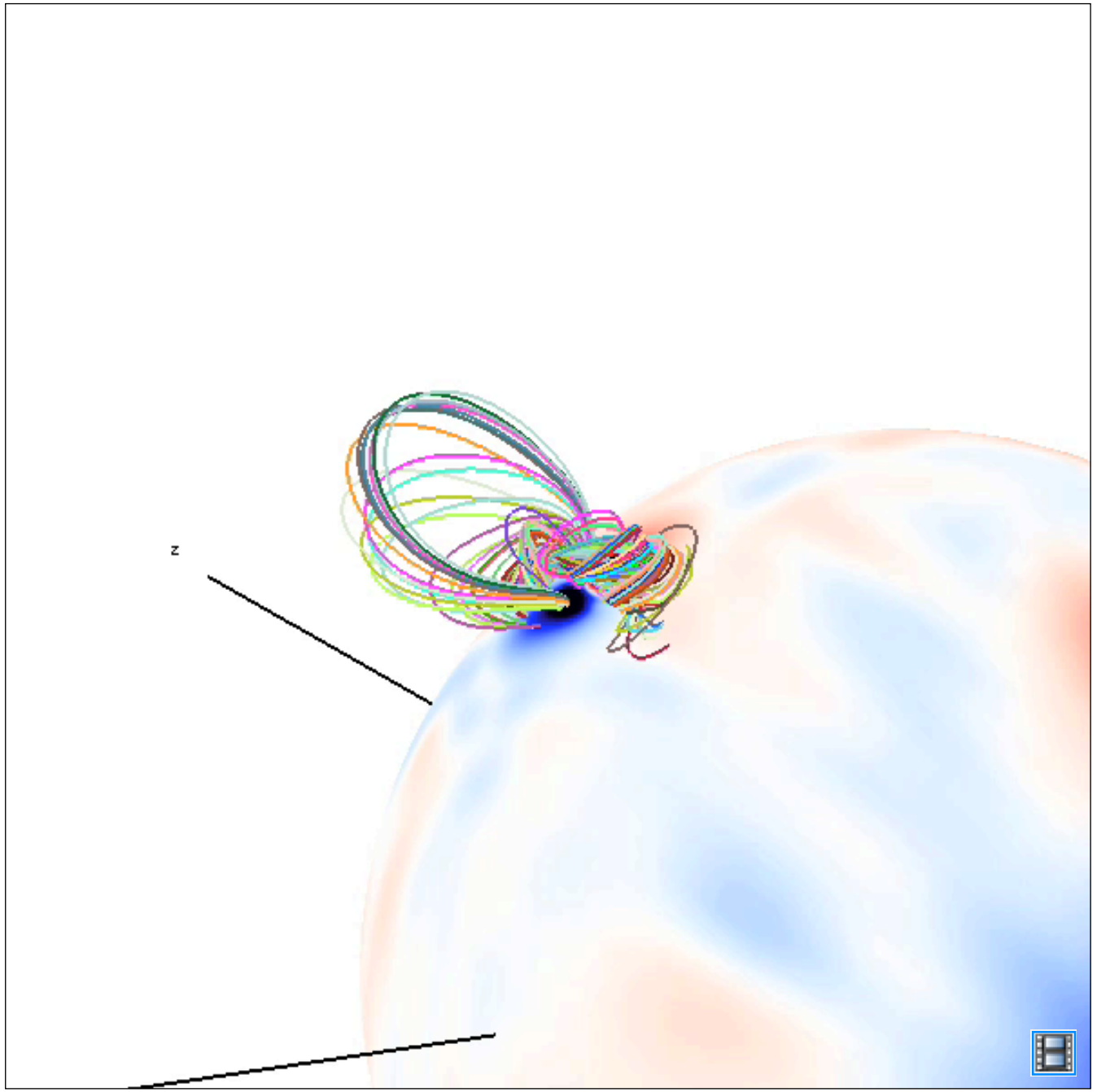

ar88dephi06

Relationship with Observational Features

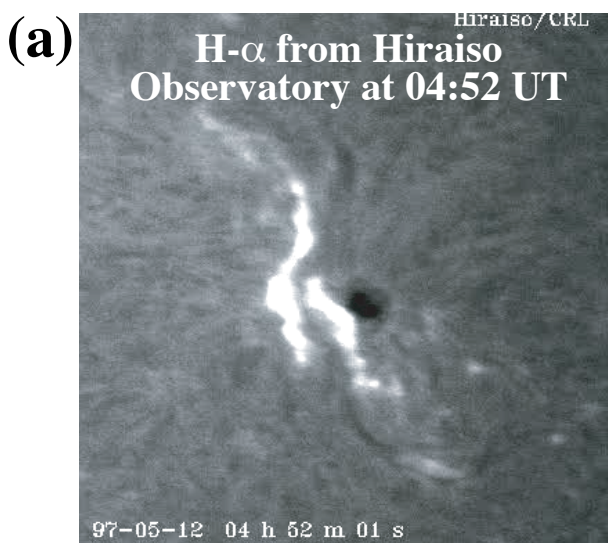

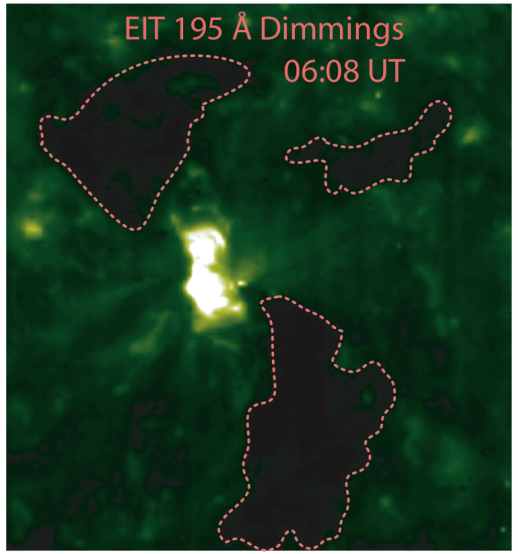

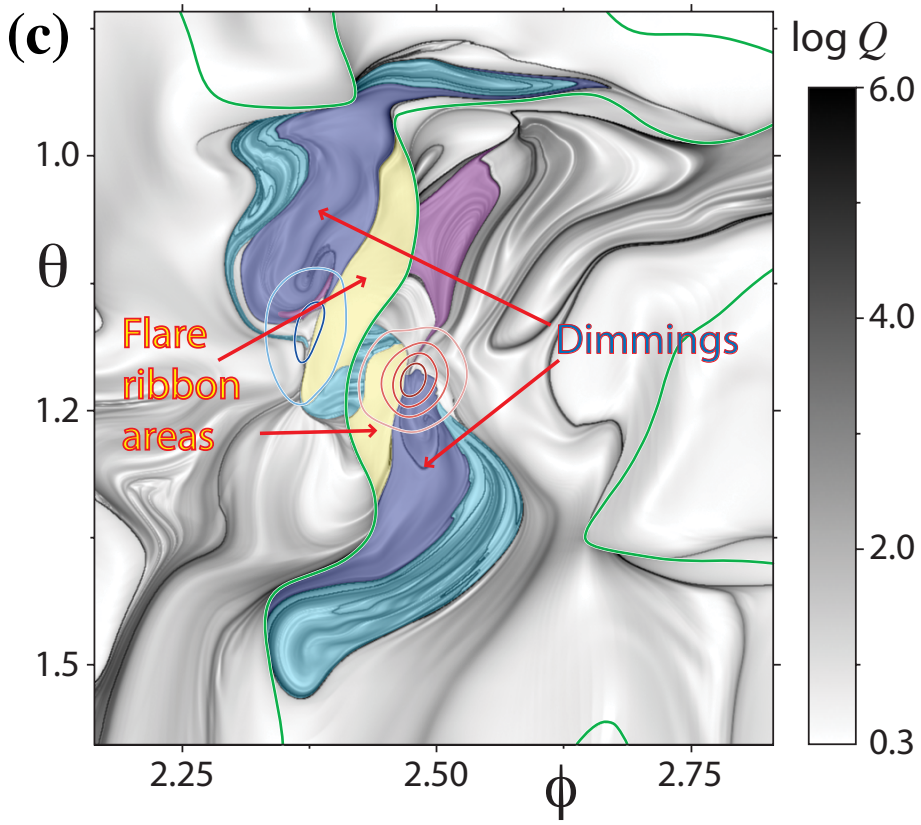

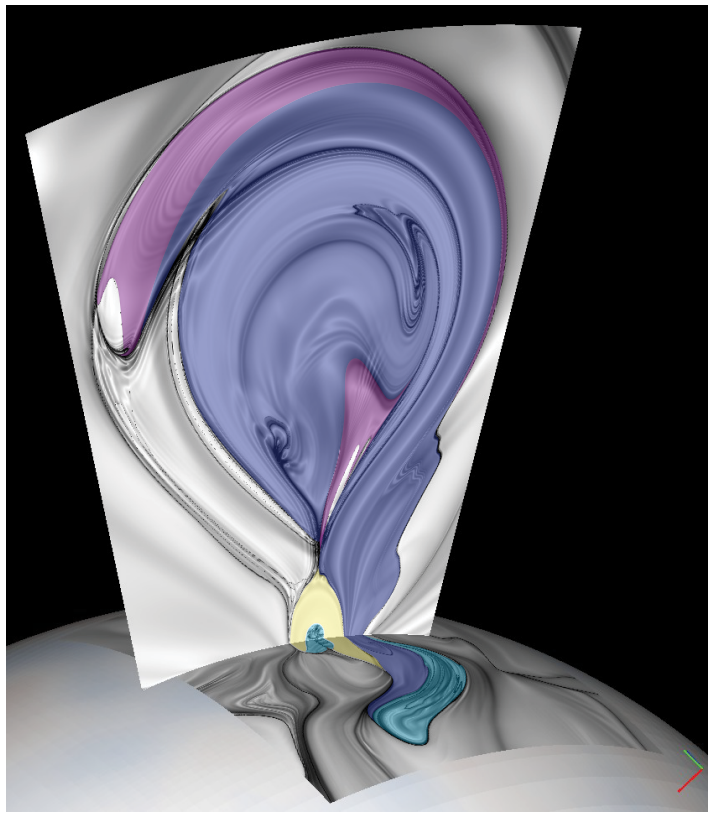

High Resolution Mesh, 151 x 228 x 323

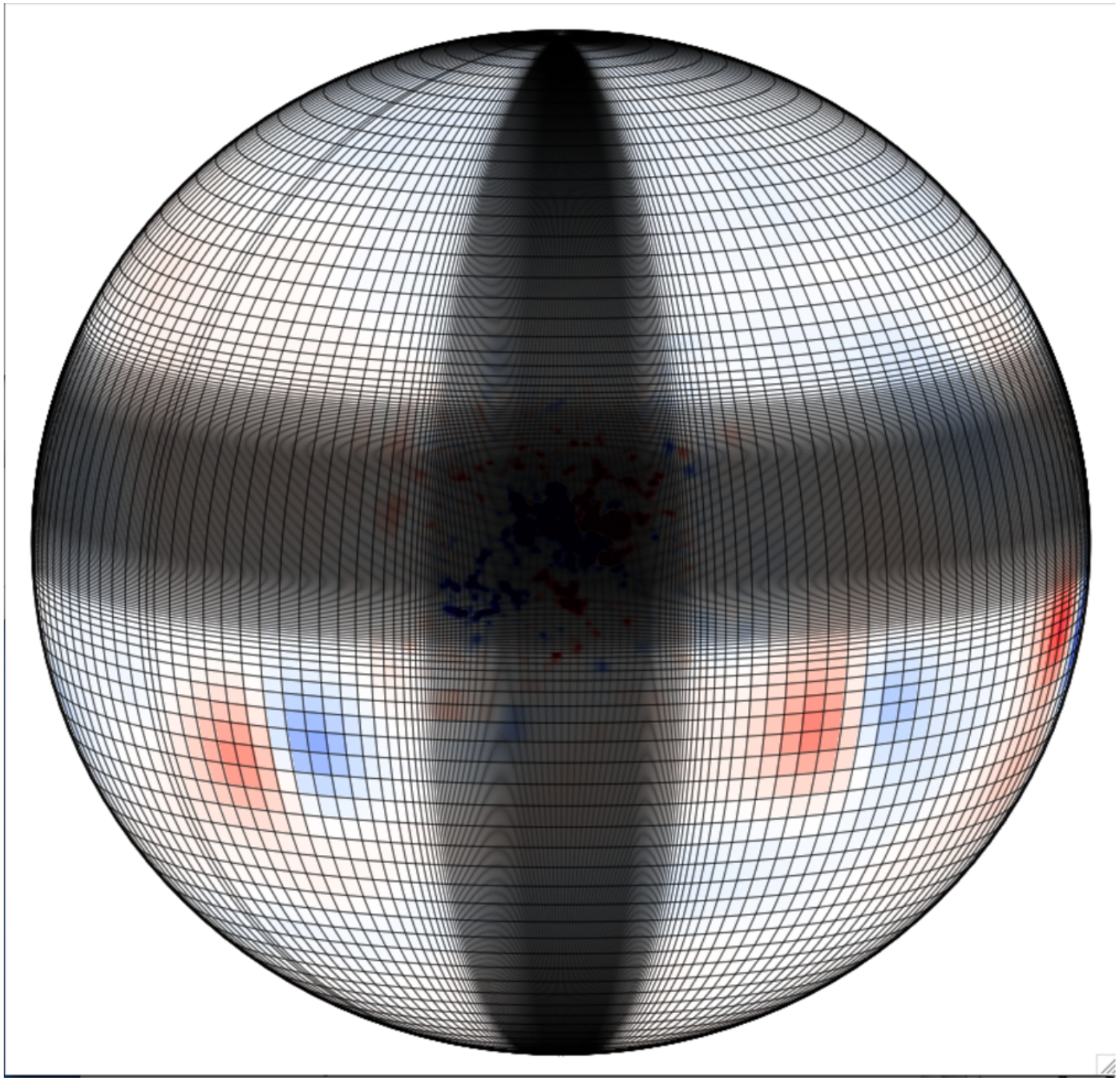

High Resolution Mesh, 151 x 228 x 323

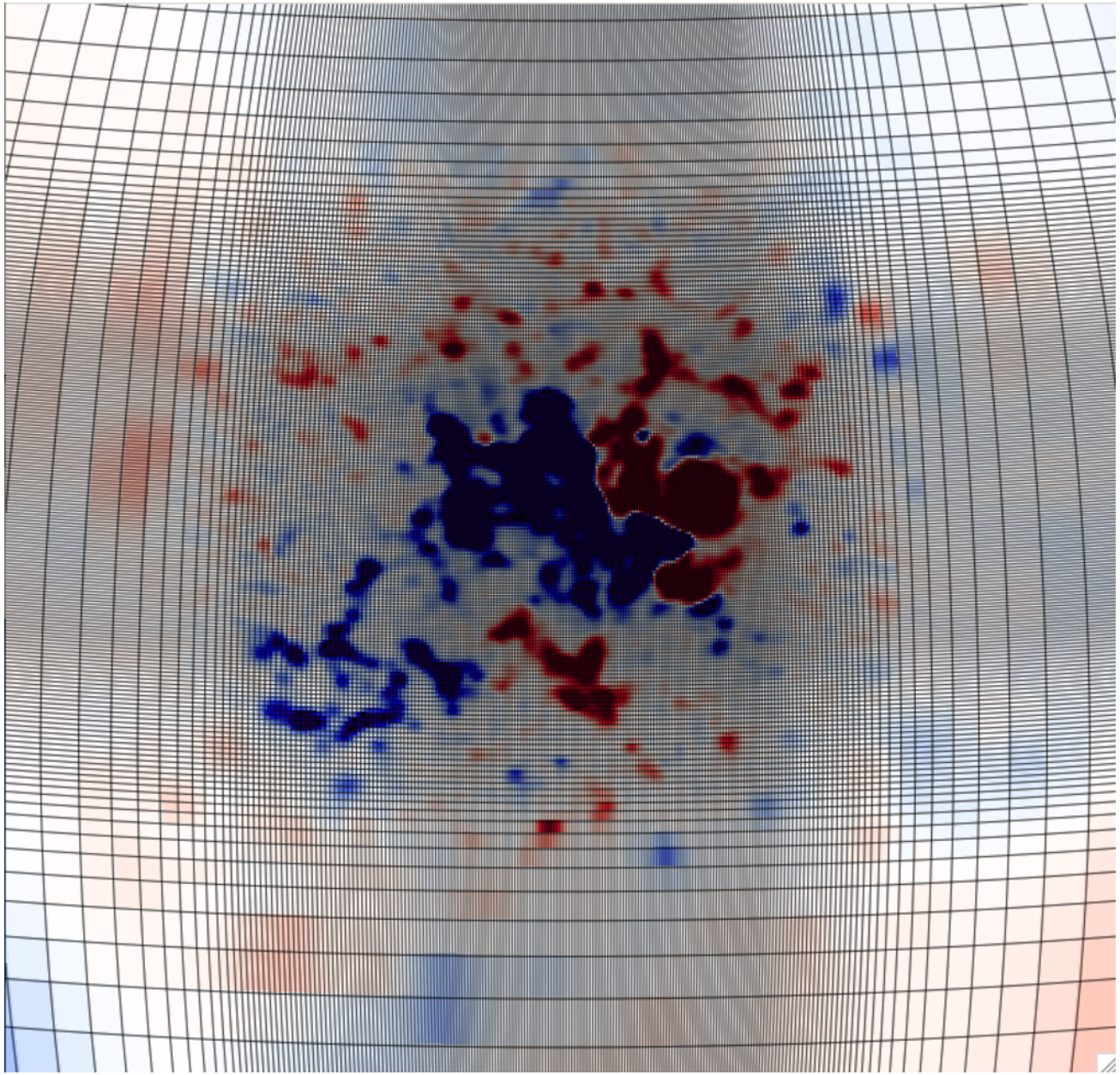

High Resolution Mesh, 151 x 228 x 323

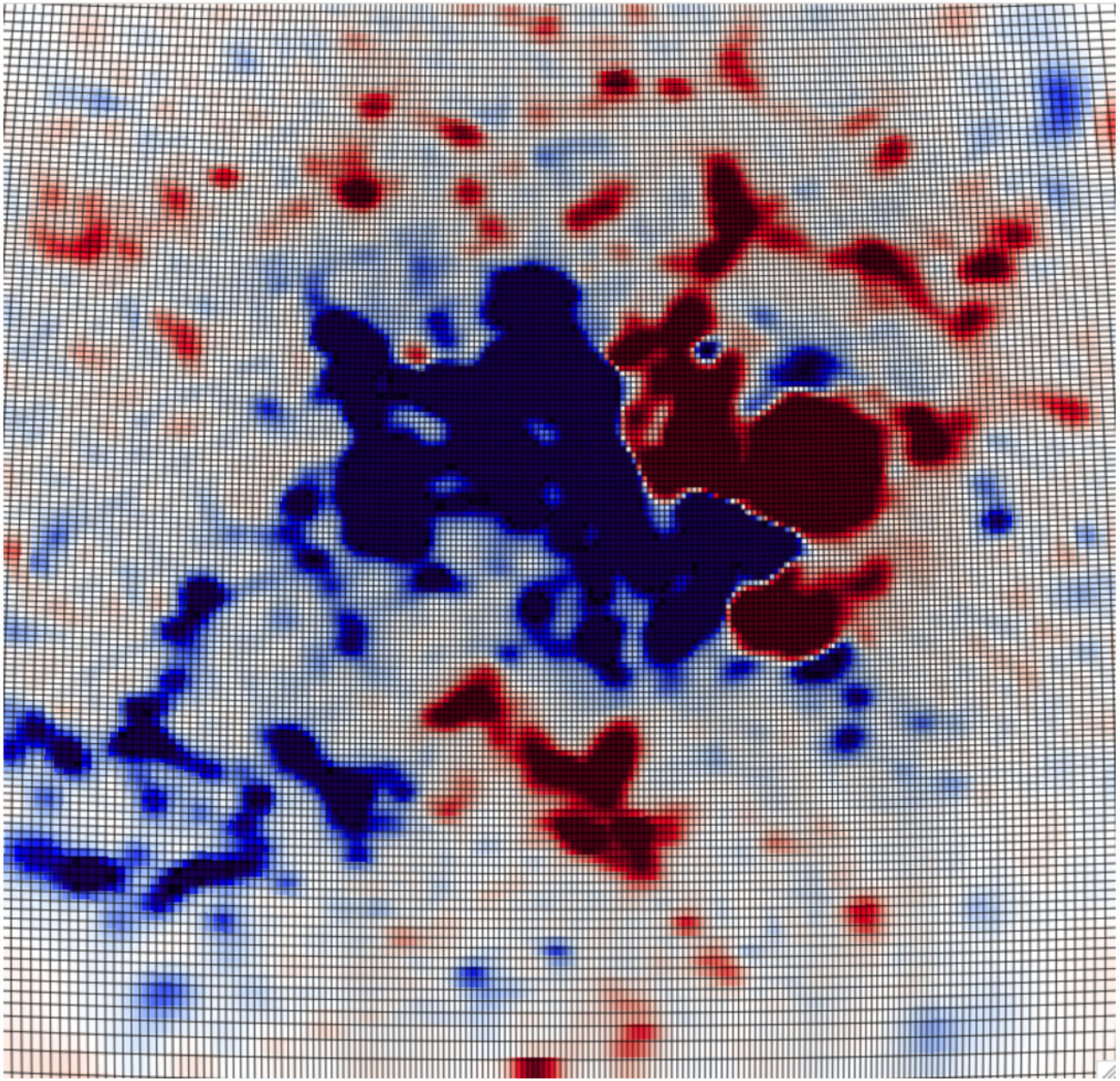

Filament Structure on May 13, 2005

ISOON H-α at ~ 16:32UT on 13 May 2005

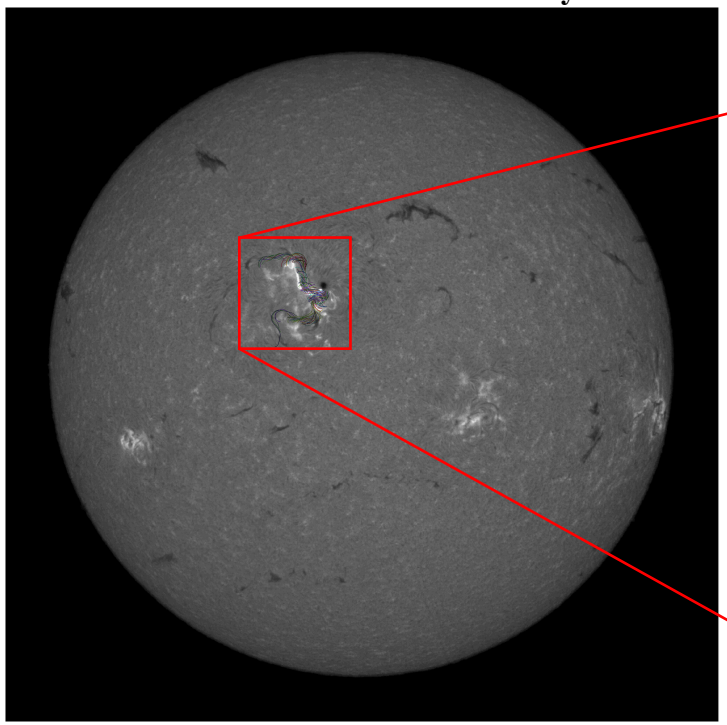

Zoomed ISOON H-α + Model Field Lines

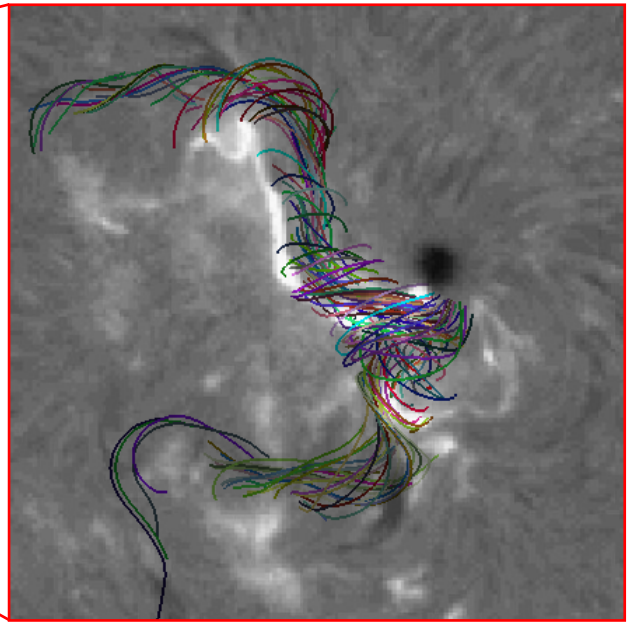

Potential Field

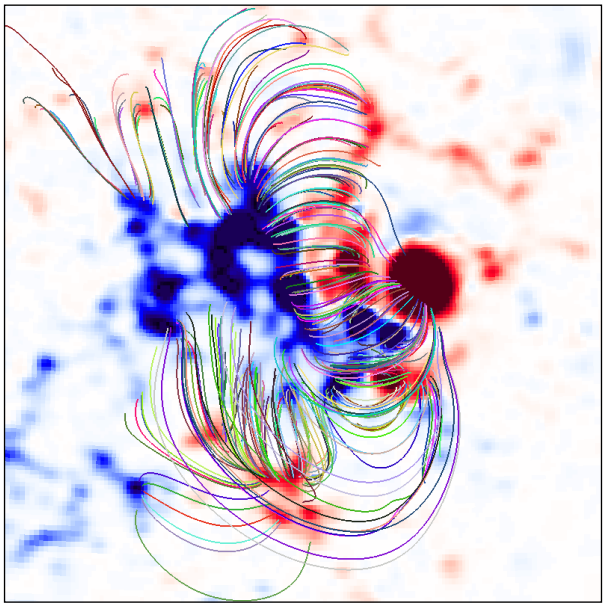

Some Emerged Transverse Field

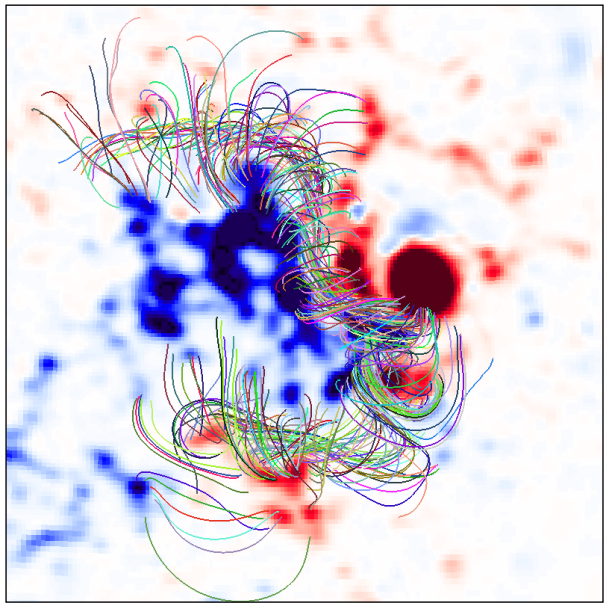

More Emerged Transverse Field

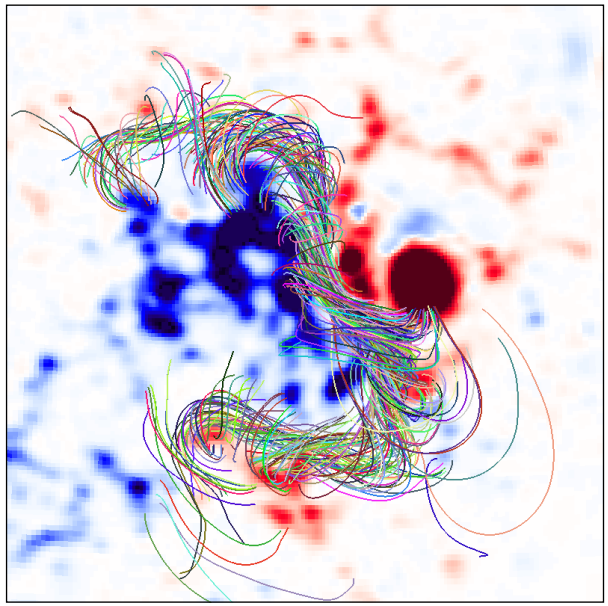

FUTURE IMPROVEMENTS (SHORT-TERM)

- More consistent treatment of magnetograms from different observatories
- Better control of smoothing of magnetograms
  - use diffusion of B_r rather than Fourier-mode and low-pass digital filtering
- Better pole-fitting
  - use time evolution of polar fields
- Allow more parameters to be varied (e.g., source-surface radius in WSA model, parameters of MHD model)
- Allow thermodynamic MAS model runs
  - currently only the polytropic model can be run at CCMC, though the thermodynamic model is already in version 4.2
  - need to finalize a "standard" coronal heating specification (difficult)
- Provide higher-level diagnostics (e.g., simulated pB and coronal emission, coronal hole maps, solar wind source regions)

FUTURE IMPROVEMENTS (LONG-TERM)

- Incorporate SDO data (HMI magnetograms, simulated emission diagnostics to compare with AIA)
- Incorporate *evolution* of photospheric fields
- Use a more fundamental coronal heating formulation: self-consistent coronal heating and solar wind acceleration from an input of waves and their subsequent dissipation (e.g., Cranmer & van Ballegooijen 2003, 2005; Cranmer *et al*. 2007; Verdini & Velli 2007; Rappazzo *et al*. 2007, 2008; Usmanov *et al*. 2009; Cranmer 2010)
- Improve robustness via error checking and cleverer input parameter processing
- Improve the speed of the MAS model

WAVE PROPAGATION AND DISSIPATION

- Alfvén and acoustic waves are propagated into the corona by specifying a wave flux at the coronal base
- These waves interact with the plasma and dissipate in open and closed field regions, accelerating and heating the solar wind
- Split the wave energy density field $\varepsilon = <\delta B^2>/4\pi$ into two fields ε_+ and ε_-:

$$\frac{\partial \varepsilon_+}{\partial t} + \nabla \cdot \mathbf{F}_+ = \tfrac{1}{2}\mathbf{v} \cdot \nabla \varepsilon_+ - \frac{C\alpha \varepsilon_+^{3/2}}{L_\perp} - D(\varepsilon_+ \varepsilon_-)^n$$

$$\frac{\partial \varepsilon_-}{\partial t} + \nabla \cdot \mathbf{F}_- = \tfrac{1}{2}\mathbf{v} \cdot \nabla \varepsilon_- - \frac{C\alpha \varepsilon_-^{3/2}}{L_\perp} - D(\varepsilon_+ \varepsilon_-)^n$$

- There are corresponding terms in the energy equation that heat the plasma

- The wave fluxes are:

$$\mathbf{F}_+ = (\tfrac{3}{2}\mathbf{v} + v_A\hat{\mathbf{b}})\varepsilon_+$$

$$\mathbf{F}_- = (\tfrac{3}{2}\mathbf{v} - v_A\hat{\mathbf{b}})\varepsilon_-$$

- The total wave energy density is given by $\varepsilon = \varepsilon_+ + \varepsilon_-$
- The wave pressure is $p_w = \frac{1}{2}\varepsilon$

POSSIBLE PITFALLS

- Magnetograms can have quality problems:
  - *subtle*: saturation effects, noise, bias and offsets, polar field oddities, processing anomalies, inter-calibration
  - *not so subtle*: missing data, partial data coverage
- There is a tendency to use magnetograms in a "black box" mode
- This can be misleading and can lead to incorrect physics conclusions
- To address this, Pete Riley has organized a series of "Magnetogram Workshops" (3 held so far) in which data producers (MDI, WSO, NSO, and MWO staff) and users exchanged experiences in detail
- We need more of these kinds of detailed interactions

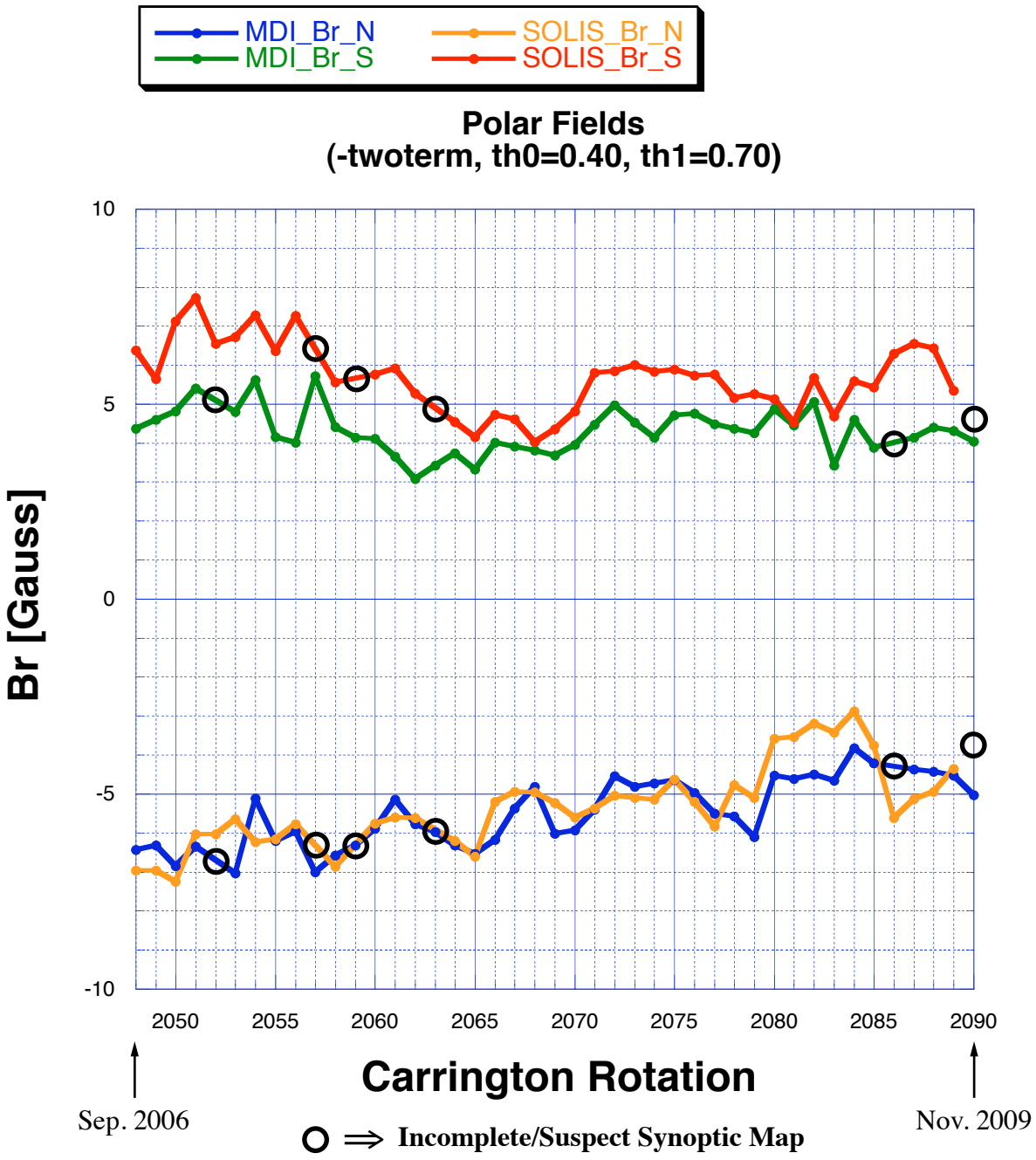
MDI_Br_N
MDI_Br_S
SOLIS_Br_N
SOLIS_Br_S
Polar Fields
(-twoterm, th0=0.40, th1=0.70)
Br [Gauss]
10
5
0
-5
-10
2050
2055
2060
2065
2070
2075
2080
2085
2090
Carrington Rotation
Sep. 2006
Nov. 2009
⇒ Incomplete/Suspect Synoptic Map

CONCLUSIONS

- We have had a long and fruitful collaboration with CCMC (~ 7 years)
- We expect this to continue
- We have successfully delivered research models to the community
- User feedback has led to model improvements and more flexible implementations at CCMC
- We expect increasingly more sophisticated applications of our models in the future (e.g., to address STEREO and SDO data)
- We are looking to implement CME models, though this is very challenging
- We need to find the right balance between robustness, flexibility, and ease of use